Plutonic-squishy lid: a new global tectonic regime generated by intrusive magmatism on Earth-like planets

Diogo L. Lourenço[1,2,3*], Antoine B. Rozel[1], Maxim D. Ballmer[1,4], and Paul J. Tackley[1]

[1]Institute of Geophysics, Department of Earth Sciences, ETH Zurich, Zurich, Switzerland
[2]University of California Davis, Department of Earth and Planetary Sciences, Davis, CA, United States
[3]University of California Berkeley, Department of Earth and Planetary Science, Berkeley, CA, United States
[4]Department of Earth Sciences, University College London, London, United Kingdom

Key Points:

- High intrusion efficiencies lead to a new global tectonic regime, named plutonic-squishy lid.
- The new regime is characterized by significant surface velocities, a thin lithosphere, and small plates.
- The new regime has the potential to be applicable to the Archean Earth and Venus.

*Current address: University of California Berkeley, Department of Earth and Planetary Science, Berkeley, CA, United States

Corresponding author: Diogo L. Lourenço, dlourenco@berkeley.edu

Abstract

The thermal and chemical evolution of rocky planets is controlled by their surface tectonics and magmatic processes. On Earth, magmatism is dominated by plutonism/intrusion vs. volcanism/extrusion. However, the role of plutonism on planetary tectonics and long-term evolution of rocky planets has not been systematically studied. We use numerical simulations to systematically investigate the effect of plutonism combined with eruptive volcanism. At low-to-intermediate intrusion efficiencies, results reproduce the three common tectonic/convective regimes as are usually obtained in simulations using a visco-plastic rheology: stagnant-lid (a one-plate planet), episodic (where the lithosphere is usually stagnant and sometimes overturns into the mantle), and mobile-lid (similar to plate tectonics). At high intrusion efficiencies, we observe a new additional regime called "plutonic-squishy lid". This regime is characterised by a set of small, strong plates separated by warm and weak regions generated by plutonism. Eclogitic drippings and lithospheric delaminations often occur close to these weak regions, which leads to significant surface velocities towards the focus of delamination, even if subduction is not active. The location of the plate boundaries is strongly time-dependent and mainly occurs in regions of magma intrusion, leading to small, ephemeral plates. The plutonic-squishy-lid regime is also distinctive from other regimes because it generates a thin lithosphere, which results in high conductive heat fluxes and lower internal mantle temperatures when compared to a stagnant lid. This regime has the potential to be applicable to the Early Archean Earth and present-day Venus, as it combines elements of both protoplate tectonic and vertical tectonic models.

Plain Language Summary

The evolution of Earth-like planets is controlled by the dynamics of their rigid outer part, called the lithosphere, and magmatic processes. Studies of terrestrial magmatic processes show that most melt is intruded into the crust. However, the effect of intrusive magmatism on the long-term evolution of rocky planets has not been systematically studied. Here we use numerical models to simulate global mantle convection in a rocky planet. When eruptions dominate, our results reproduce the three tectonic regimes found in previous studies: mobile lid, similar to plate tectonics operating on modern-day Earth, stagnant lid or a planet covered by a single plate, and episodic lid where the planet is covered by one plate that resurfaces into the mantle more or less frequently. For high intrusion efficiencies, we describe the new "plutonic-squishy-lid" regime. Hot intrusions make the lithosphere squishy and lead to drippings and delaminations of the crust. In turn, these processes lead to significant surface velocities (even if subduction is not active), and small, short-lived plates. The lithosphere is kept thin and therefore the loss of heat from the interior is efficient. The new regime has the potential to be applicable to the Archean Earth and Venus.

1 Introduction

The surface tectonics of a planet reflects its dynamics, and controls long-term cooling and planetary evolution. Some of the terrestrial planets in the Solar System show little or no evidence of surface motion, likely being covered by a thick and non-yielding lithosphere, known as a "stagnant lid" (Nataf & Richter, 1982; Christensen, 1984; Solomatov, 1995). In contrast, the Earth is characterized by relative surface motion between lithospheric plates that are continuously recycled back into the mantle, in a regime known as a "mobile lid" (Tackley, 2000; Stein, Schmalzl, & Hansen, 2004). A mobile lid, equivalent to plate tectonics in numerical models, implies active subduction, a process characterized by the descent of oceanic lithosphere as a coherent slab into the mantle due to its negative buoyancy (e.g., Bédard, 2018). Venus, in turn, has been proposed to be in an "episodic lid" regime, characterised by bursts of surface mobility due to episodic

overturns of an unstable stagnant lid (Turcotte, 1993; Moresi & Solomatov, 1998; Noack, Breuer, & Spohn, 2012; Rozel, 2012; Armann & Tackley, 2012) or internal mantle instabilities (Davies, 1995; Bédard, 2018), although continuous, random resurfacing may also match cratering statistics (O'Rourke, Wolf, & Ehlmann, 2014). In this work, we define an overturn or a resurfacing event as the process where all or almost all of the lithosphere of a planet descends into the mantle in a short period of time. (Lourenço et al. (2016) found that the timescale for such an event is on the order of 20-25 million years). A fourth global tectonic regime, the "ridge-only" regime, where discrete zones of plate divergence (ridges) can appear in the lithosphere without generating subduction zones, has been reported and may apply to the early Earth and icy satellites (Tackley, 2000; Rozel, Golabek, Naef, & Tackley, 2015). The key factors that control global-scale planetary tectonics through time remain to be understood (Weller & Lenardic, 2012).

A mobile-lid convection regime with plate-like behavior can be modelled numerically using strongly temperature-dependent viscosity and plastic yielding (Fowler, 1993; Moresi & Solomatov, 1998; Tackley, 2000; Stein et al., 2004). In these models, a maximal "yield" stress, at which the lithosphere "breaks" into plates, is imposed. This critical yield stress necessary to obtain mobile-lid behaviour in numerical simulations is much smaller than what is estimated from rock-deformation experiments (Kohlstedt, Evans, & Mackwell, 1995). This discrepancy occurs due to several factors that remain under active debate. For example, whereas numerical models typically focus on purely thermal convection, compositional variations in the lithosphere can produce density anomalies, which in turn generate non-negligible additional stresses (Lourenço et al., 2016). Mechanisms that have been found to facilitate plate tectonics include: the presence of water (Regenauer-lieb, Yuen, & Branlund, 2001; Hirth & Kohlstedt, 2003; Dymkova & Gerya, 2013), the presence of continents (Rolf & Tackley, 2011), magmatic weakening (Sizova, Gerya, Brown, & Perchuk, 2010; Gerya, Stern, Baes, Sobolev, & Whattam, 2015), and melting-induced crustal production (Lourenço et al., 2016). The spatial resolution of the discretization of the domain used to compute deformation can also play an important role in facilitating plate tectonics in numerical models (Gerya et al., 2015).

In a recent work by Lourenço et al. (2016), it was shown that Earth-like plate tectonics is more likely to occur in planets where a crust of variable thickness and different density is produced by partial melting and eruption. This conclusion was reached after comparing global mantle convection numerical simulations with and without melting and crustal production. The authors employed a first-order approximation by assuming that all magmatism was extrusive. However, this is not the case in the Earth (Crisp, 1984; Cawood, Hawkesworth, & Dhuime, 2013) and other Earth-like bodies such as Venus (Gerya, 2014).

In this article, we extend the work of Lourenço et al. (2016) by taking into account intrusive magmatism. We present a set of 2D spherical annulus simulations of mantle convection (Hernlund & Tackley, 2008) considering different intrusion *versus* extrusion efficiencies. We focus on the effects that intrusive magmatism may have on the tectonic regimes of Earth-like planets. We first describe our model in section 2. In section 3 we present our results, which are analysed in section 4 and discussed in section 5. Finally, in section 6 we present the conclusions of this study.

2 Model and method

The model used in this study is based on the one described by Lourenço et al. (2016). The model incorporates realistic parameter values and physics descriptive of planet Earth, and thus includes compressibility, phase transitions, pressure-temperature-dependence of viscosity, time-dependent internal and basal heating, and plasticity. Several assumptions and simplifications are employed in this study. The depth-dependent yield stress envelope is simplified into an effective single value that represents the strength of the litho-

sphere on tens of kilometers length scales as generally used in global mantle convection studies. Furthermore, a simplified melting model is used, particularly in terms of Archean melting.

2.1 Rheology

Diffusion creep, with the assumption of homogeneous grain size, is the assumed viscous deformation mechanism. It follows a temperature- and pressure-dependent Arrhenius law:

$$\eta_{\text{diff}}(T,p) = \eta_0 \exp\left(\frac{E+pV}{RT} - \frac{E}{RT_0}\right), \tag{1}$$

where η_0 is the reference viscosity at zero pressure and reference temperature T_0 (= 1600 K), E is the activation energy, p is the pressure, V is the activation volume, T is the absolute temperature and R is the gas constant. Different values for E and V are used for the upper mantle, lower mantle and post-perovskite, and furthermore V decreases with pressure to give profiles consistent with Karato and Wu (1993) and Yamazaki and Karato (2001). Two sets of simulations are presented in this work, using two different reference viscosity (η_0) values, 10^{20} and 10^{21} Pa·s.

It is assumed that the material deforms plastically after reaching a yield stress, σ_{y}, defined as:

$$\sigma_{\text{y}} = \sigma_{\text{duct}} + \sigma'_{\text{duct}}\, p, \tag{2}$$

where σ_{duct} is the surface ductile yield stress and σ'_{duct} is the vertical gradient of the ductile yield stress. In practice, this last parameter prevents plastic yielding in the deep mantle. The parameter with the greatest influence in the previous equation is σ_{duct}, and is therefore the second parameter that we vary in our study. We use values between 20 and 300 MPa, in intervals of 20 MPa. The definition of the yield stress used here is commonly used in global mantle convection studies and simplifies the depth-dependent yield stress envelope into an effective strength of the lithosphere on tens of kilometers length scales. This is a way to transform a complex multi-parameter yield envelope into a one-parameter average stress value. Using a more complex Byerlee expression would not affect our results as the resolution that can be used in global long-term evolutionary models is limited. The relatively low resolution and simplified rheological mechanisms considered in global models, such as in this study, can also help to explain the discrepancy between yield stress values used in geodynamical studies and the higher values inferred from laboratory deformation studies (e.g., Kohlstedt et al., 1995).

The effective viscosity, combining diffusion creep (Eq. 1) and plastic yielding (Eq. 2), is given by:

$$\eta_{\text{eff}} = \left(\frac{1}{\eta_{\text{diff}}} + \frac{2\dot{\varepsilon}}{\sigma_{\text{y}}}\right)^{-1}, \tag{3}$$

where $\dot{\varepsilon}$ is the second invariant of the strain rate tensor. The viscosity is not directly dependent on melt fraction or composition. However, it is strongly temperature dependent (see Eq. 1).

2.2 Phase changes, composition and melting-induced crustal production

A parameterisation based on mineral physics data (e.g., Irifune & Ringwood, 1993; Ono, Ito, & Katsura, 2001) is included in the model, dividing minerals into the olivine and pyroxene-garnet systems, which undergo different solid-solid phase transitions, as used in previous studies (Xie & Tackley, 2004; Nakagawa & Tackley, 2012). The mixture of minerals depends on the chemical composition, which varies between two end-members: basalt (pure pyroxene-garnet) and harzburgite (75% olivine). Accordingly, our

simplified parameterization limits the degree of depletion to harzburgitic residues under any conditions. While this assumption might not always hold for the hotter Archean mantle, the global heat and material fluxes are not strongly affected.

Pressure- and temperature-dependent solid-solid phase transitions occur in both the pyroxene-garnet and the olivine phase systems. The depths, reference temperatures, density jumps and Clapeyron slopes of each phase change are detailed in Table 2 of Lourenço et al. (2016). The importance of the eclogite phase transition, which occurs in the pyroxene-garnet phase system, should be emphasized. We consider that basalt becomes eclogite at a depth of 60 km, leading to a 350 kg/m^3 density increase, most often in the lithosphere. A large amount of basalt erupted to the surface might therefore destabilize the lithosphere if the eclogite phase transition is reached, and the lithosphere is deformable enough, which depends on its temperature profile (Lourenço et al., 2016).

As in previous studies (e.g., Xie & Tackley, 2004; Nakagawa, Tackley, Deschamps, & Connolly, 2010; Lourenço et al., 2016), changes in composition arise from melt-induced differentiation. At each time step, the temperature in each cell is compared to the solidus temperature as used by Nakagawa and Tackley (2004), which is a function that fits experimental data by Herzberg et al. (2000) in the upper mantle and by Zerr et al. (1998) in the lower mantle. If the temperature in a specific cell exceeds the solidus then enough eclogitic melt is generated in order to bring the temperature back to solidus, leaving a more depleted residue behind depending on the degree of melt generated. Melting can only occur if the material is not completely depleted. The generated melt is then emplaced in the form of extrusive volcanics or intrusive plutons, in a predefined proportion, and always with a basaltic composition. It is assumed that the percolation of melt through the solid mantle is much faster than convection (Condomines, Hemond, & Allègre, 1988). Thus, part of the shallow melt is instantly removed and extruded to the surface to form oceanic crust with the surface temperature, while the rest is intruded at the base of the crust, as suggested by Vogt et al. (2012). An important difference between these two modes is that the extruded magma immediately loses the heat it carries (i.e. both latent heat and sensible heat) to the atmosphere/hydrosphere, while intruded magma carries its heat to the place where it is emplaced. A higher intrusion to extrusion ratio leads to a warmer, less viscous lid. Adiabatic heating and cooling are considered for magma moving upwards or downwards during magmatic processes.

In order to study the effects of intrusion on the convection regime and overall evolution of a rocky planet, we run simulations with intrusion efficiencies (I) of 0, 10, 20, 30, 50, 70 and 90%. The melt that is not intruded is erupted. Therefore, the eruption efficiency (E) is:

$$\mathrm{E}(\%) = 100 - \mathrm{I}(\%). \tag{4}$$

Crust is only produced from melts above the depth of neutral buoyancy, which is $\sim$ 300 km on Earth. Due to technical difficulties, we did not compute models accounting for 100% intrusive magmatism. Future studies should aim to explore this limit.

Using a strongly temperature-dependent rheology (Eq. 1), as expected in the plate tectonics paradigm and confirmed by deformation experiments, leads to the formation of a mechanical boundary layer, the lithosphere (Turcotte & Schubert, 2014). The lithosphere should not be confused with the crust, a compositional layer, which in our model arises from melting processes. The thickness of the crust is computed from the cell-based composition field. Its value may vary depending on the vigor of convection, i.e., the crust can either be protected by the lithosphere (typically when the viscosity of the upper mantle is high) or eroded by the mantle flow. When intrusive magmatism dominates, it generally leads to a warming-up of the crust (and therefore the lithosphere), which can self-consistently promote delamination events.

2.3 Radiogenic heating

Radioactive decay of heat-producing elements in the crust and mantle leads to internal heating. The radiogenic heating rate per unit mass is assumed to decay exponentially with time and to be spatially uniform. Heat-producing elements concentration is assumed to have the "bulk silicate Earth" value of 5.2×10^{-12} W/kg at present day, and an average half-life of 2.43 Gyr (Sun & McDonough, 1989). This means that the internal heating initial value is 18.77×10^{-12} W/kg. Segregation of heat-producing elements into the crust is not included in this study.

2.4 Effective thermal conductivity for magma

The initial potential temperature in the simulations presented in this work is 1917 K, an adequate initial temperature to study the Earth's evolution starting from the Precambrian (Jaupart, Labrosse, & Mareschal, 2007; Herzberg, Condie, & Korenaga, 2010; Johnson, Brown, Kaus, & VanTongeren, 2014). Due to the higher temperature in the planet's mantle and due to intrusion, pockets of high melt fraction are expected in and around the newly intruded crust. Largely molten silicates have very low viscosities, in the order of $\eta_{\mathrm{liq-sil}} \sim 0.1{-}100$ Pa·s (Abe, 1993; Costa, Caricchi, & Bagdassarov, 2009), which leads to very efficient cooling when compared to a mostly-solid rock. To simulate this fast cooling in the modelled (geological) timescales, an effective thermal conductivity method is employed for high fractions of magma. We parameterise the heat flux, J_{q}, as previously done in other studies (Abe, 1993, 1997):

$$J_{\mathrm{q}} = -k_{\mathrm{h}} \left[\frac{\partial T}{\partial r} - \left(\frac{\partial T}{\partial r} \right)_{\mathrm{s}} \right] - k \frac{\partial T}{\partial r}, \tag{5}$$

where k is the thermal conductivity, k_{h} is the effective thermal conductivity, $(\partial T/\partial r)_{\mathrm{s}}$ is the adiabatic temperature gradient and r is the radius of the planet. k_{h} is a function of the melt fraction, and its value is 10^5 W/(m.K) for melt fractions $\phi > 60\%$, a negligible value (≈ 0) when $\phi < 20\%$, and an hyperbolic tangent step function in-between ~ 0 and 10^5 W/(m.K) when $20\% \geq \phi \leq 60\%$ (see Fig.S1). This smooth step function reflects the fact that when the melt fraction in a partially-molten rock is higher than a certain critical value, generally taken as $\sim 40\%$, solid particles are disconnected and the viscosity is controlled by that of the melt (Arzi, 1978; Abe, 1993; Costa et al., 2009). In practice, k_{h} implies that low-viscosity high-melt-fraction molten rocks transport heat 5 orders of magnitude faster than solid rock, as the maximum value of k_{h} is 10^5 W/(m.K), and k, the thermal conductivity of a lithospheric solid rock is typically a value around 3 W/(m.K).

2.5 Boundary conditions and solution method

The physical model is solved using the numerical code StagYY (Tackley, 2008) in a two-dimensional spherical annulus (Hernlund & Tackley, 2008). StagYY uses a finite-volume discretisation of the governing compressible anelastic Stokes equations (e.g., Schubert, Turcotte, & Olson, 2001). Tracers are used to track composition and to allow for the treatment of partial melting and crustal formation. Crustal material produces density anomalies which enter the right hand side of the Stokes equation in addition to the thermal density anomalies. A direct solver is employed to obtain a solution of the Stokes and continuity equations, using the PETSc toolkit (Balay et al. (2012); `http://www.mcs.anl.gov/petsc`). The heat equation is solved in two steps: advection is performed using the MPDATA scheme and diffusion is then solved implicitly using a PETSc solver. Free-slip boundary conditions are employed at the surface and core-mantle boundary to address the thermochemical evolution of Earth over 4.5 billion years. The temperature at the surface is fixed to 300 K. Core cooling is included, based on the works by Buffett et al. (1992) and Buffett et al. (1996). Details on the parameterisation used for core cooling can be found in Nakagawa and Tackley (2004). The computational domain is decom-

posed in 512x64 cells, in which around one million tracers are advected. For simplicity, dimensional units are used throughout this study. Furthermore, time in our models is forward running, which means that 4.5 Gyr is present-day.

3 Results

Over the years, numerical simulations run using different codes and employing different degrees of complexity have provided consistent results: in general, when a visco-plastic, strongly temperature-dependent rheology is used, three convective regimes with different surface expressions are found. These are: mobile lid for low yield stresses, episodic lid for intermediate yield stresses and stagnant lid for high yield stresses (Moresi & Solomatov, 1998; Tackley, 2000; O'Neill, Jellinek, & Lenardic, 2007; Nakagawa & Tackley, 2015; Lourenço et al., 2016). Fig. 1 shows the mantle final thermal and compositional states of one example of these regimes, obtained through the simulations run in the present study (Fig. 1C depicts a new regime described later in this work). A mobile lid (Fig. 1A) is characterized by permanent surface velocities of the order of a few cm/yr mostly due to active subduction. The sinking of large slabs forces large-scale deformation in the mantle, which enhances mixing and produces thin boundary layers leading to high conductive heat flow. On the other end of the spectrum, a planet covered by a stagnant lid has negligible surface velocities. Internal convection still operates, but as no subduction occurs and the planet generally has a thick crust, the heat loss is less efficient than in a mobile-lid regime, leading to a relatively warm mantle (Fig. 1D). Between the two end members, an episodic lid is characterized by the occasional mechanical resurfacing of the lid, made possible by a moderate yield stress, too high to allow for a mobile lid but too low to sustain a stagnant lid. Overturns are characterized by very high surface velocities, and negligible surface velocities are reported between overturns. During the fast overturns of the lid, heat loss is very efficient, which leads to intermediate mantle temperatures compared with the previous two regimes (Fig. 1B). In this work we want to systematically explore the boundaries between the different regimes and the controlling parameters that define these boundaries, in particular testing the effect of intrusive magmatism. Our approach is to run a large number of simulations and classify them into a regime in a quantitative way. This is what we do next.

3.1 Mobility

We start by defining a quantitative measure of lithosphere activity, which we apply in order to analyse the results: the Mobility (M), which represents the extent to which the lithosphere is able to move in a given time frame, when compared to the mantle. If velocities of the lithosphere are comparable with the mantle, then subduction is active, and mobility is high. If velocities of the surface are negligible when compared with the mantle, then the lithosphere is stagnant (stagnant-lid regime). M is computed according to Tackley (2000), and is defined as the ratio of the root mean square (rms) of the surface velocity averaged over the rms velocity of the entire computational domain (all cells):

$$M = \frac{(\nu_{\mathrm{rms}})_{\mathrm{surface}}}{(\nu_{\mathrm{rms}})_{\mathrm{mantle}}}. \tag{6}$$

$M \approx 1$ for constant-viscosity, internally heated convection (in which the top boundary layer is mobile but not plate-like), meaning that the surface velocities are equivalent to the interior velocities. M can be greater than 1 in a mobile-lid case as the lithosphere is pulled by downgoing slabs, which gives the surface a slightly larger velocity than the average velocity in the entire domain. For stagnant-lid cases, M is near zero, as surface velocities are negligible. During resurfacing events in an episodic-lid regime M can reach 1 but is sometimes smaller, depending on the thermal and compositional state of

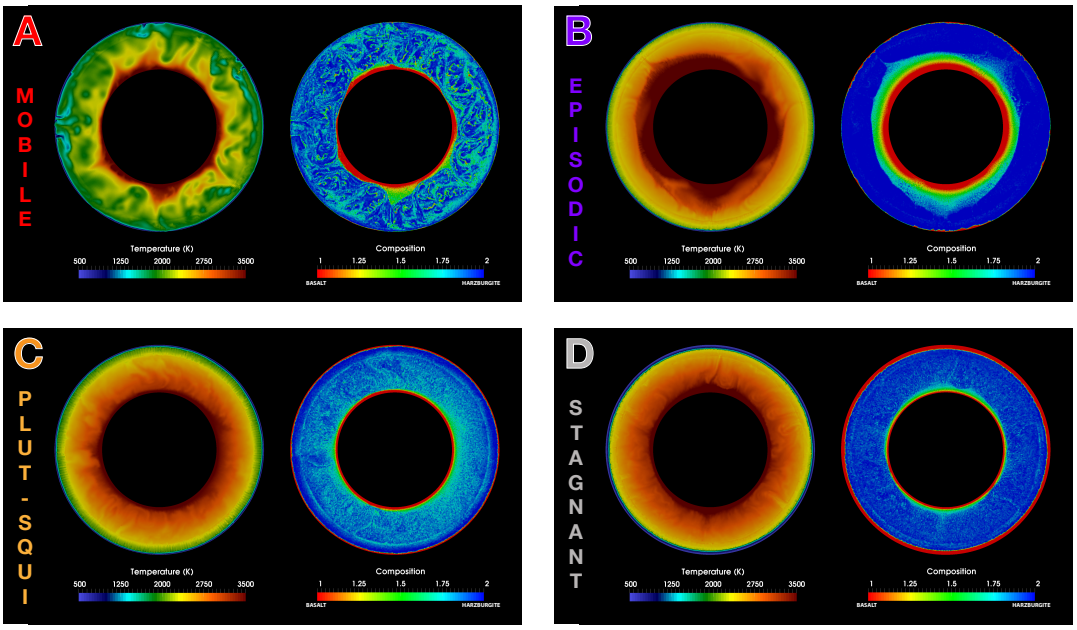

Figure 1: Final temperature and composition states, at 4.5 Gyr of the evolution of four different cases for which $\eta_0 = 10^{21}$ Pa·s. The regimes are (A) mobile lid (surface yield stress (σ_{duct}) = 20 MPa, eruption efficiency (E)= 10%), (B) episodic lid (σ_{duct} = 100 MPa, E = 70%), (C) Plutonic-squishy-lid (σ_{duct} = 300 MPa, E = 10%), and (D) stagnant lid σ_{duct} = 300 MPa, E = 100%). It is important to note that, even if these cases depict typical final states of different convective regimes, there can be variation within cases in the same regime. Composition ranges from 1 (basalt, in red) to 2 (harzburgite, in dark blue).

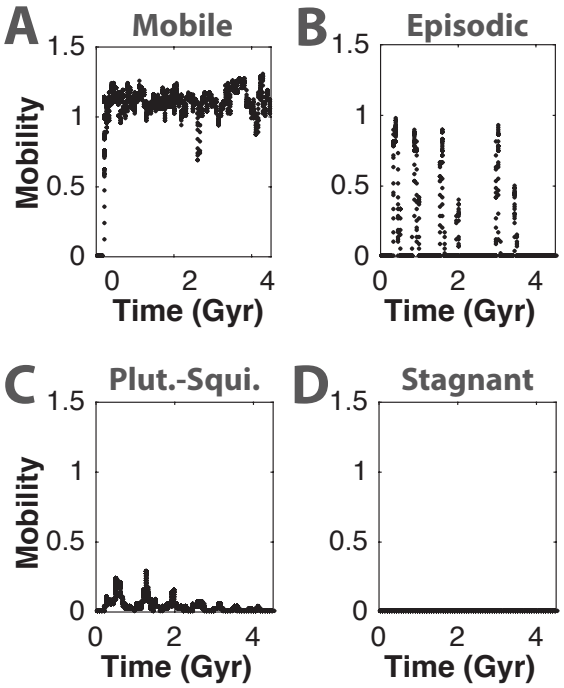

Figure 2: Mobility over time for the same four cases as in Fig.1: (A) mobile lid (plate tectonics), (B) episodic lid, (C) plutonic-squishy lid, and (D) stagnant lid.

the planet. Examples of M through time during the evolution of models with different tectonic regimes are shown in Fig. 2 for four selected cases.

Fig. 3 shows the time-averages of the mobility from 0 to 4.5 Gyr for all simulations. Two sets of simulations with different reference viscosities, η_0, are shown: $10^{20} Pa{\cdot}s$ in Fig. 3A, and $10^{21} Pa \cdot s$ in Fig. 3B. For both cases a mobile-lid regime is obtained at low yield stresses (yellow to green background representing high mobility values over time), where plasticity is dominant in the lithosphere and a stagnant lid can never form. A stagnant lid (the dark-blue shaded region) is obtained at high yield stresses because naturally developing convective stresses remain lower than the yield stress. However, this is only true for extrusion efficiencies higher than 20% for $\eta_0 = 10^{20}$ Pa·s, and 10% for $\eta_0 = 10^{21}$ Pa·s. At 80-90% intrusion efficiency (therefore 10-20% extrusion efficiency), which is the range expected for the Earth (Crisp, 1984), there is a dramatic change: a stagnant lid does not exist anymore. For intermediate and high yield stress and low eruption efficiency (the light-blue shaded area in the diagrams in Fig. 3), intermediate mobility values are obtained.

3.2 Surface velocity

In order to better understand the different tectonic regimes present in the model results, the surface velocities for both η_0 are plotted as a function of time in Fig. 4. The surface velocities strongly depend on the reference viscosity used: velocities are higher for lower viscosities. This is consistent with scaling laws based on boundary layer theory such as $v \propto \eta\,(T_\mathrm{i})^{-2/3}$ (Schubert et al., 2001), where $\eta\,(T_\mathrm{i})$ is the effective viscosity based on the internal temperature T_i.

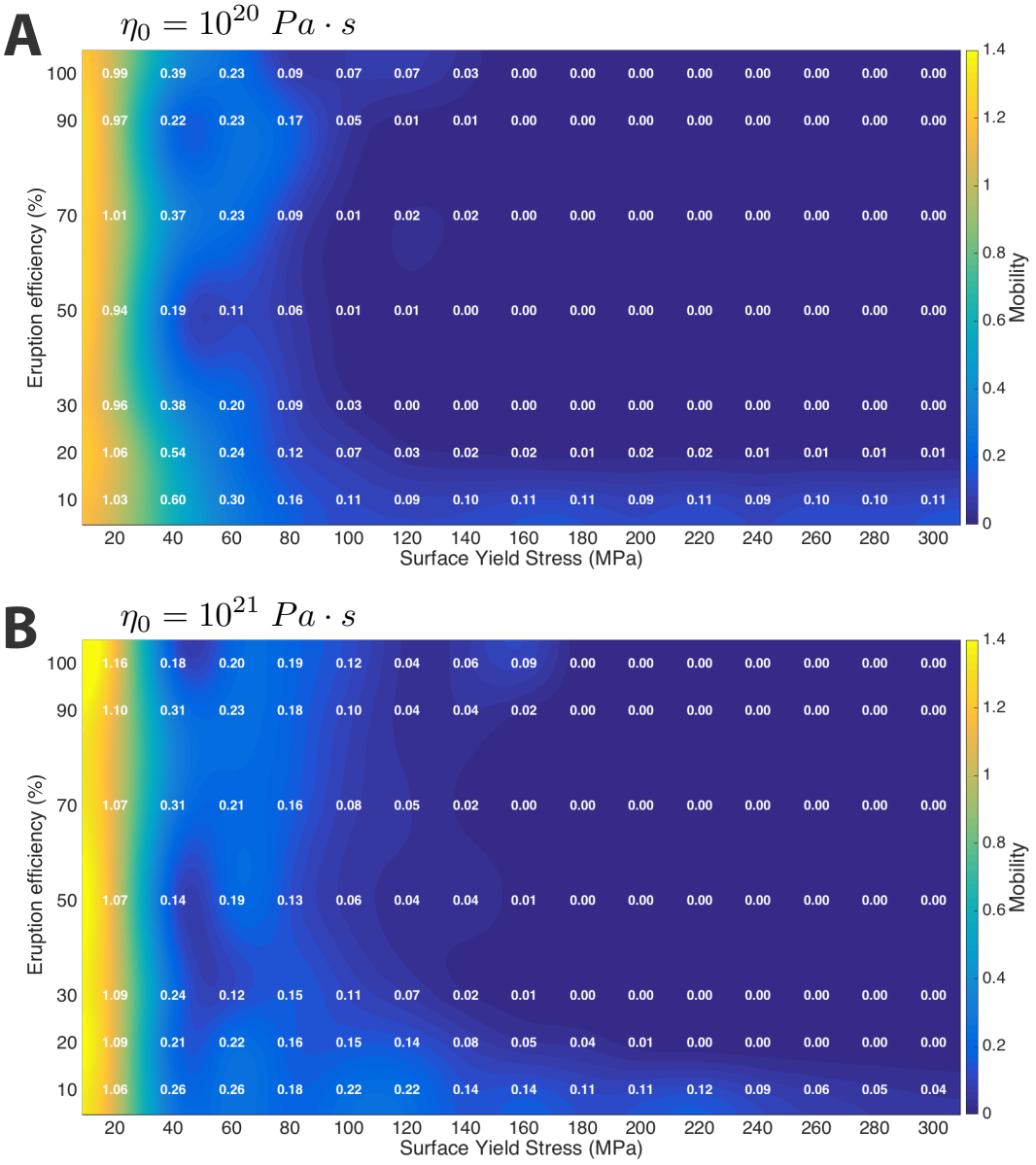

Figure 3: Mobility as a function of yield strength and eruption efficiency for cases with a reference viscosity of: (A) 10^{20}, and (B) 10^{21} Pa·s. The value represents the mobility averaged in time from 0 to 4.5 Gyr. Each number inside the diagrams represents one computation.

For high yield stresses and eruption efficiencies higher than 10−20%, surface velocities are minimal throughout the whole evolution of the planet, a characteristic of the stagnant-lid regime. In contrast, low yield stress cases result in mobilities of more than 0.5 (see yellow region in Fig. 3). These simulations are characterised by non-negligible surface velocities that at first oscillate around high values, and later stabilise with time as the planet cools down, with values of a few cm/yr. These velocities are consistent with a mobile-lid regime. Most of the cases in a mobile-lid regime have been obtained in simulations employing a surface yield stress of 20 MPa. There are however two cases, with yield stress of 40 MPa, $\eta_0 = 10^{20}$ $Pa{\cdot}s$ and eruption efficiencies of 10 and 20%, which we classify as mobile lid but have a slightly different evolution: they show constant sinking of basaltic material, but are characterized by frequent slab break-off when compared with cases with a 20 MPa surface yield stress. This sort of "intermittent" subduction, in which a plate drips in a ductile way instead of sinking as a rigid slab, has been observed before (e.g., van Thienen, van den Berg, & Vlaar, 2004a, 2004b; van Hunen & van den Berg, 2008; Moyen & Martin, 2012; Sizova, Gerya, Stuwe, & Brown, 2015) and named "dripduction" by Moyen and Laurent (2018). These cases go through a period characterised by drippings, which are short-lived and sporadic, before undergoing a transition to smoothly-evolving plate tectonics around one billion years before the end of the simulation (present day).

A very interesting observation when looking at Fig.4 is that in the light-blue shaded areas in Fig. 3, corresponding to intermediate mobility values, different behaviours can be distinguished. A classic episodic-lid regime with sporadic and fast overturns separated by periods with negligible surface velocity exists for intermediate yield stress values. The number of overturns decreases as the surface yield stress increases, for different runs. Additionally, for high yield stress values and low eruption efficiencies, velocities of intermediate magnitudes (between mobile and stagnant-lid values) can be observed. A remarkable characteristic of this regime is that even when there is no on-going subduction (which occurs in some cases), the lid velocities almost never decrease to stagnant-lid level. The lid is always "squishy" enough, due to high intrusion efficiencies of warm material, to always be moving, though no major downwelling is able to form.

3.3 Plateness

Another measure that we use to quantitatively distinguish between planetary tectonic regimes is the plateness. Plateness is based on a fundamental characteristic of plate tectonics: rigid plates are separated by weak boundary regions in which the majority of the deformation occurs. A plate is defined in this work as an area of the lithosphere over which surface velocities are near constant and which is surrounded by areas of high deformation (plate boundaries) when compared to its interior.

We define plateness based on the works by Weinstein and Olson (1992) and Tackley (2000). The square root of the second invariant of strain rate,

$$\dot{\varepsilon}_{surf} = \frac{\dot{\varepsilon}_{\phi\phi}}{\sqrt{2}}, \tag{7}$$

is used. The total integrated $\dot{\varepsilon}_{surf}$ is calculated, followed by the fraction of the surface area in which 80% of that deformation occurs. This area fraction, denoted f_{80}, would be zero for perfect plates (meaning all deformation takes place within infinitely narrow zones). As Tackley (2000) pointed out, in isoviscous, internally heated calculations with $Ra_H = 10^6$, $f_{80} \approx 0.6$. This means that 80% of the surface deformation occurs in 60% of the surface area. As plateness should vary between 0 for homogeneous-viscosity cases and 1 for perfect plates, the definition for plateness, P, is:

$$P = 1 - \frac{f_{80}}{0.6}. \tag{8}$$

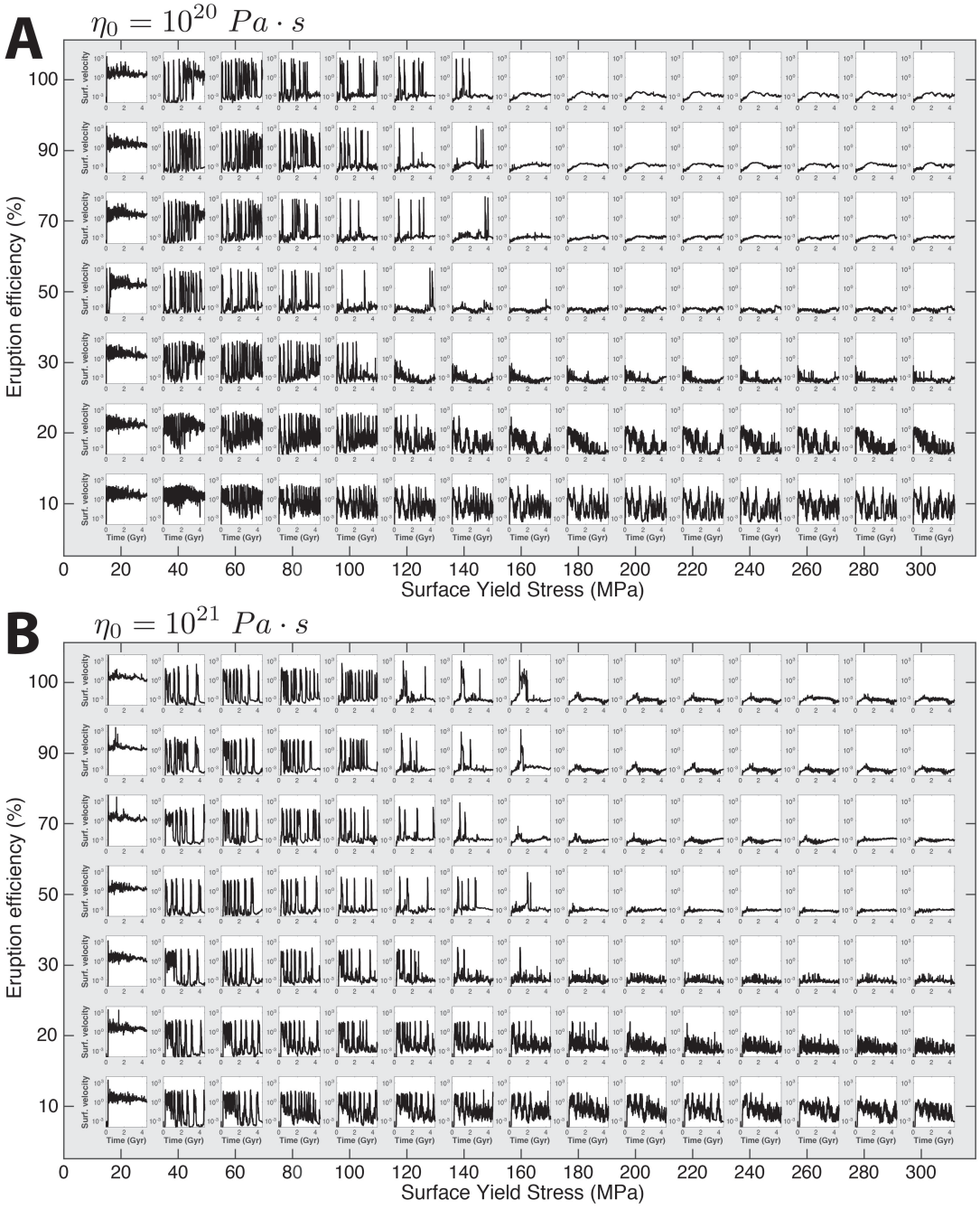

Figure 4: Surface velocity (cm/yr) in logarithmic scale as a function of time for all the numerical simulations run with a reference viscosity of: (A) 10^{20}, and (B) 10^{21} Pa·s.

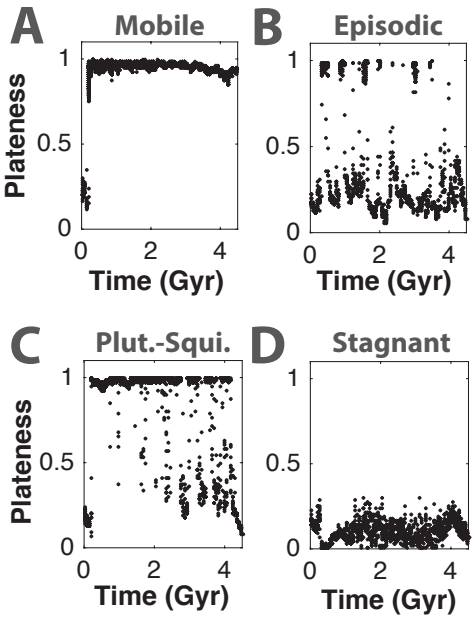

Figure 5: Plateness over time for the same four cases as in Figs. 1 and 2: (A) mobile lid (plate tectonics), (B) episodic lid, (C) plutonic-squishy lid, and (D) stagnant lid.

It is known that plate boundaries, both oceanic and continental, can be hundreds to thousands of kilometres wide (Gordon & Stein, 1992). Therefore, we should bear in mind that $P = 1$ is not strictly expected for mobile-lid cases, but should in any case be relatively high when plates exist, and rather low for a planet in a stagnant-lid regime, covered by a single plate.

The plateness through time, for the four example cases as in Fig. 2, is plotted in Fig. 5. For the mobile-lid case (Fig. 5A), $P \approx 1$ throughout most of the evolution of the planet. In the episodic-lid case (Fig. 5B), $P \approx 1$ during overturns, but otherwise remains small (≈ 0.2). For the stagnant-lid example case (Fig. 5D), P is quite low, ≈ 0.1. The plutonic-squishy-lid case, plotted in Fig. 5C, shows that even if there is no subduction and the velocities of the lid are small, there are plates throughout most of the evolution of the model. Thus, plateness allows a distinction between episodic- and plutonic-squishy-lid regimes, as the former only has short-lived plates during overturns being otherwise covered by a single plate, while the latter almost always has plates. However, another problem arises: the average P can be similar for mobile and plutonic-squishy lid. In order to isolate the latter, instead of a simple time-average of P, we calculate the average plateness throughout all the evolution of each model, but only taking into account time frames in which the average surface velocity is not significant, i.e. when it is lower than 1 cm/year, a criterion used before in Lourenço et al. (2016). We name this quantity Quiescent Plateness (QP), computed as:

$$\mathrm{QP} = \frac{1}{t_{\mathrm{tot}}} \int_{t=0}^{t=t_{\mathrm{tot}}} P(t) \cdot (1 - H(\nu_{\mathrm{surf}}(t) - 1))\, dt\,, \tag{9}$$

where ν_{surf} is the surface velocity, t_{tot} is the total simulated time (4.5 Gyr in our case), and H is an Heaviside step function:

$$H(\nu_{\mathrm{surf}}(t) - 1) = \begin{cases} 0, & \text{if } \nu_{\mathrm{surf}}(t) < 1 \\ 1, & \text{if } \nu_{\mathrm{surf}}(t) \geq 1 \end{cases}. \tag{10}$$

Therefore, P values are only accounted if $\nu_{\text{surf}}(t) < 1$. Note that QP is a plateness multiplied by the dimensionless time representing the fraction of quiet surface tectonic duration during the total evolution time of the model.

QP can be understood as an indicator of the presence of plates by measuring how focused surface deformation is (indicating plate boundaries), in a planet that does not experience active subduction. QP for all our runs is plotted in Fig. 6. We can use QP as a diagnostic for the plutonic-squishy-lid cases because: (1) mobile-lid cases predominantly display characteristic surface velocities higher than 1 cm/year, and therefore QP ≈ 0, (2) stagnant-lid cases experience small and widespread deformation, which locally re-equilibrates heterogeneous crustal loads, therefore QP is very small, (3) episodic-lid cases only have significant surface velocities during overturns, therefore QP is small ($\approx 0.2-0.3$), and finally (4) any plutonic-squishy lid, even if there might be some episodicity, is characterised by plate-like behaviour at relatively small surface velocities, therefore QP ≥ 0.4 (this is the value of the isocontour plotted in Fig. 6). Using Mobility and Quiescent Plateness as diagnostics we can now isolate the different tectonic regimes obtained in the numerical simulations presented in this work.

3.4 Tectonic Regimes

We have identified four tectonic regimes so far: mobile, episodic, plutonic-squishy, and stagnant. However, it is important to make a further distinction: a stagnant-lid case with an extrusion efficiency of 100% (and where the main mode of heat loss is through magmatism, rather than conduction through the lithosphere) is defined as being in a heat-pipe regime. This (sub-)regime has been proposed to be important for the early Earth (Moore & Webb, 2013) and for Io, a moon of Jupiter (O'Reilly & Davies, 1981). This regime was also taken into account when building the regime diagram shown in Fig. 7, which pinpoints the parameter space where the various tectonic regimes are active for a reference viscosity of $10^{20}\ Pa \cdot s$ in Fig. 7A and $10^{21}\ Pa \cdot s$ in Fig. 7B. The criteria to build this regime diagram are the following: (1) a mobile-lid regime exists if the averaged mobility value over the 4.5 Gyr of evolution (shown in Fig. 3) is more than 0.5, (2) a stagnant-lid regime exists if the averaged mobility in time is lower than $5 \cdot 10^{-3}$ (i.e., labelled "0.00" in Fig. 3), (3) if the criterion described in the previous point is true and if the eruption efficiency is 100%, then the regime is specifically classified as a heat pipe, (4) a plutonic-squishy-lid regime exists if the quiescent plateness value is higher or equal to 0.4, and (5) if the average mobility is a value between $5{\cdot}10^{-3}$ and 0.5 and if the quiescent plateness value is less than 0.4, then an episodic-lid regime exists.

In general we can say that: (1) A mobile lid is expected for low yield stresses. Therefore on Earth, where plate tectonics exists, the key factor is the low stresses at which the surface rocks yield, together with an oceanic lithosphere that is cold and stiff enough to drive subduction. Higher intrusion efficiencies can play a role in facilitating plate tectonics by making the lithosphere weaker, as shown in Fig. 7(A) for a surface yield stress of 40 MPa and eruption efficiencies lower than 25%. (2) An episodic lid is expected for intermediate yield stress values (40 - 180 MPa depending on the eruption efficiency and reference viscosity) and eruption efficiencies higher than 10-20% (for a few cases 30%). The transition from an episodic-lid to a stagnant-lid regime occurs at higher yield stress values for a higher reference viscosity. This is an expected behaviour, which is in agreement with analytically predicted critical yield stress obtained with boundary layer theory (Solomatov, 2004; Lourenço et al., 2016). For the lower reference viscosity tested in this study, $10^{20}\ Pa \cdot s$, the effect of the eruption efficiency is evident: more volcanism replaces a stagnant lid with an episodic lid, as the crust extends beyond the depth of the eclogite phase change. However, for the higher reference viscosity tested, $10^{21}\ Pa \cdot s$, the effects of the eruption efficiency are more complex: an episodic-lid is more likely for intermediate eruption efficiencies (i.e., 70%). The cause for this is discussed later in section 4.1. (3) A stagnant lid is expected for high yield stresses and eruption efficiencies

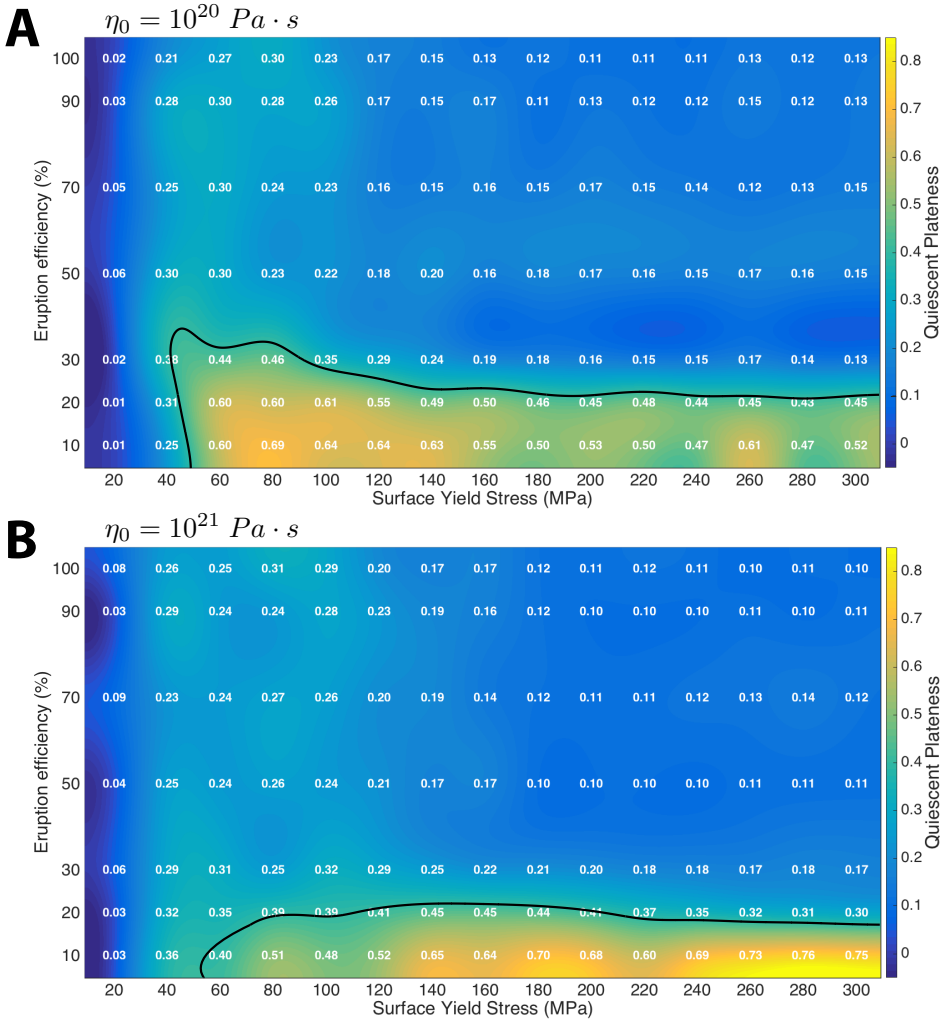

Figure 6: Diagram in the parameter space of yield strength and extrusion efficiency for cases with a reference viscosity of: (A) 10^{20}, and (B) 10^{21} Pa·s. Each number inside the diagrams represents one computation. The value represents the Quiescent Plateness (QP), computed as the average plateness integrated in time for each model, but only taking into account time frames where the surface velocity is smaller than 1 cm/year. The solid black line is the QP=0.4 isocontour. If QP $\geq$ 0.4 the tectonic regime is identified as a plutonic-squishy lid.

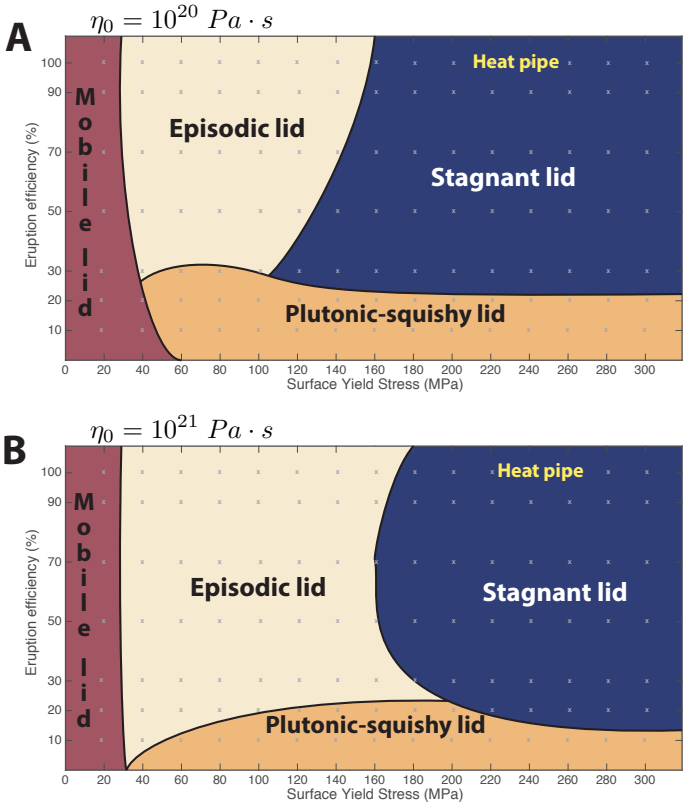

Figure 7: Regime diagram in the parameter space of yield stress and eruption efficiency, for a reference viscosity of: (A) 10^{20}, and (B) 10^{21} Pa·s. See text for details on how the different regimes are defined.

higher than 10% for a $\eta_0 = 10^{21}\ Pa \cdot s$, or 20% for a $\eta_0 = 10^{20}\ Pa \cdot s$. (4) The newly found plutonic-squishy-lid regime is expected for yield stress values higher than 50 MPa and eruption efficiencies lower than 20 - 30% depending on the reference viscosity. A detailed description of the plutonic-squishy-lid regime, and the way it operates, is presented next.

3.5 Plutonic-squishy-lid regime

Figs. 8 and 9 depict how a planet in a plutonic-squishy-lid regime operates and the processes that lead to movement in the lid. Fig. 8 shows a time evolution of a zoomed-in portion of the crust and mantle from one of our simulations. Fig. 9 shows a more readable interpretation of what can be seen in Fig. 8, though it is also based on more observations at various other time steps, and different cases.

The top row of Fig. 8 depicts velocity and it is possible to see how a plutonic-squishy lid is characterized by a lithosphere divided into several short-lived plates, whose size is ultimately controlled by upper-mantle convection currents and related thermal anomalies. Zones of weaknesses and extension are related to warm mantle upwellings, while zones of convergence and dripping are related to downwellings. The short-lived plates move at different velocities, which can be as high as several cm/yr for one particular plate. These significant lid velocities (without subduction), and the existence of plates are related to intrusive magmatism, which has not been taken into account in the past. However, understanding what is responsible for plate motion, characterized by movement towards

or away from bordering plates, is not straightforward. Compositional anomalies are formed in the lithosphere due to eruption-intrusion processes. We also observe that magmatic intrusions do weaken the lithosphere due to the temperature-dependence of the viscosity. Therefore, it is hard to know if it is the intruda itself that drives plate motion, or if the thermally weakened intrusion sites are the factor allowing for plate motion, in turn driven by compositional anomalies located elsewhere in the plate. Key processes in a plutonic-squishy lid are shown in Fig. 8 and highlighted by sets of symbols A1-4, B1-4 and C1-4.

Fig. 9 depicts schematically the typical evolution of a plutonic-squishy lid: (A) Several plates exist, separated by hot and weak boundaries due to intrusive magmatism. A lithospheric drip starts to develop due to the fact that the material is warm and partially molten. (B) As the drip detaches from the lithosphere and sinks into the asthenosphere it causes a return flow. The material going up experiences decompression melting, and as the melt rises, a small portion erupts and the rest is intruded at the base of the crust. The intruded material leads to a rise in temperature in this portion of the crust, and thus a localized weakening that causes the localization of a new zone of deformation. The old plate boundary (in blue) disappears and the plate now extends to the new boundary (in green). A cold drip starts forming. (C) As the cold drip detaches, it also generates a return flow, which leads to melting and in a similar manner as before, to a new plate boundary. The plate in blue is now shortened. These processes keep occurring through time, creating and erasing short-lived plate boundaries and driving plate motion. Their timescales are generally a few million years. The position and size of the warm lithospheric anomalies are determined by the return flow from the mantle. Therefore, the viscosity of the upper mantle might play an important role in the localization of these short-lived plate boundaries. A lower viscosity will tend to produce more intense and localized magmatic intrusions. In 2D, intrusions directly lead to plate boundaries, however one can expect that localized intrusions should connect to each other to form more diffuse plate boundaries in 3D.

In summary, a plutonic-squishy lid is characterised by significant surface velocities in some plates even if subduction is not active, frequent lithospheric delaminations, and strong plates separated by weak boundaries due to plutonism (Fig. 8 and Fig. 9). Key requirements for the existence of a plutonic-squishy lid are high intrusion efficiencies, high mantle temperatures and the phase change from basalt to eclogite. The plutonic-squishy-lid regime resembles the plume-lid tectonics regime observed by Sizova et al. (2010) and more recently by Fischer and Gerya (2016a), both in regional models, in an attempt to model Archean tectonics. This resemblance is further discussed in section 5.1.

4 Analysis

Different convection regimes have been extensively studied and scaling analysis of them widely performed (e.g., Fowler, 1985; Solomatov, 1995; Reese, Solomatov, & Moresi, 1998; Solomatov, 2004; Valencia & O'Connell, 2009; van Heck & Tackley, 2011; Foley & Bercovici, 2014). However, almost all of these studies focus on purely thermal convection. An effort to understand the influence of melting and crustal production was made in the work by Lourenço et al. (2016). In the present paper, we extend this work and report for the first time the impact of the intrusion efficiency (as a complement to eruption) on the global evolution of Earth-like planets, through a systematic study. In this section we analyse the effects of intrusive magmatism on the mobility of the lid, internal temperatures and how the enrichment (or depletion) in basaltic material affects the thermal evolution and heat flows of the convecting mantle.

For more information and analytical scaling of the impact of intrusion on several quantities, such as internal temperature, heat flow, eruption rate and several compositional measures, the reader is referred to the Supplementary Material.

4.1 Mobility of the lid

As shown in the previous section, the first-order effect of intrusive magmatism is to increase the mobility of the lid. A higher intrusion to extrusion ratio can extend the time in the evolution of the planet during which a smoothly evolving mobile lid is present, as can be seen in Fig. 7A for a surface yield stress of 40 MPa. Most importantly, at high intrusion efficiencies, a stagnant lid can be replaced by a plutonic-squishy lid, which presents significant mobility without modern-day style subduction. For a lower reference viscosity of 10^{20} $Pa{\cdot}s$, the parameter range in which an episodic lid exists increases with increasing extrusion efficiency. This happens because higher eruption efficiencies tend to result in greater crustal thicknesses that can provide an additional negative buoyancy force due to eclogitization (Lourenço et al., 2016). For a higher reference viscosity of 10^{21} $Pa \cdot s$ the same process happens for high and intermediate eruption efficiencies. However, low eruption efficiencies also facilitate the breaking of a stagnant lid, replacing it with an episodic lid. This shows that there is an interplay between two effects: the thickening of the crust due to volcanism, and the weakening of the crust caused by delaminations and eclogitic drips due to plutonism. Both of these processes help in breaking the lid. In general, the weakening of the crust due to plutonism seems to be more important for a larger parameter range. However, when both these processes are important they tend to neutralize each other leading to a more stable lithosphere for intermediate intrusion/eruption efficiencies.

4.2 Internal temperature

The internal temperatures of all cases run are shown in Fig. 10. The internal temperature is computed as the interior temperature averaged over the 200 km below the point of minimum viscosity in the upper mantle and the last half billion years of evolution for each case. This approach samples the final thermal state of the upper mantle, which can be in turn linked to the crust and the lithosphere final states. In Fig. 10, the internal temperatures are plotted as a function of the surface yield stress for both reference viscosities tested (10^{20} $Pa \cdot s$ in Fig. 10A, and 10^{21} $Pa \cdot s$ in Fig. 10B). The results obtained follow a similar pattern for both reference viscosities. In general, final internal temperatures are highest for stagnant-lid cases and lowest for mobile-lid cases, with squishy-lid and episodic-lid cases in between. Thus, the mobile-lid regime (obtained mostly for yield stresses of 20 MPa) is the most efficient at cooling the mantle. Within the episodic-lid regime, internal temperatures increase with increasing yield stress, reflecting the decreasing frequency of resurfacing. Within the plutonic-squishy-lid regime, internal temperatures slightly decrease with increasing yield stress and do not signifi-

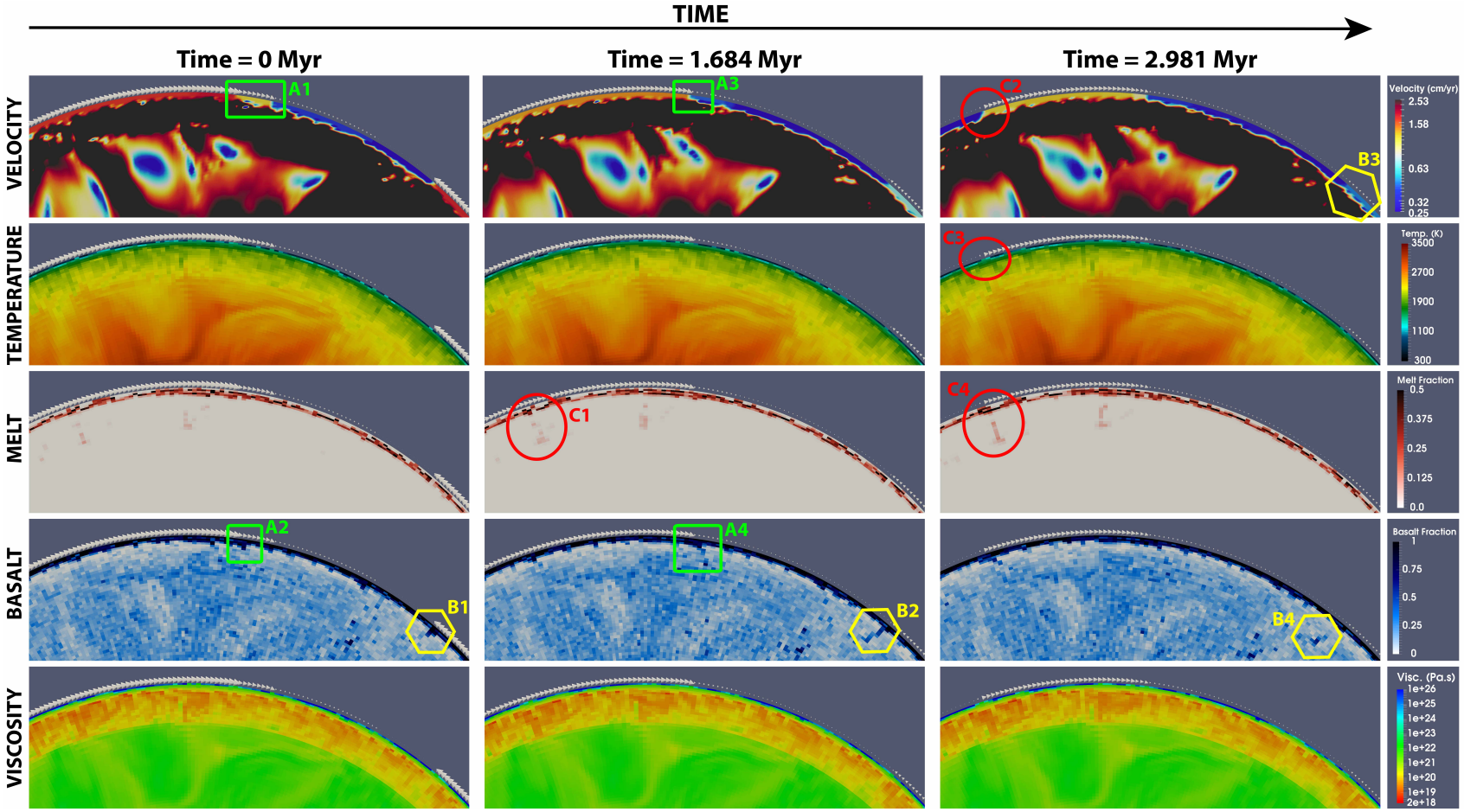

Figure 8: Dynamics of a plutonic-squishy lid (in this simulation $\eta_0 = 10^{21}$ Pa·s, $\sigma_{duct} = 300$ MPa and I=90%). Three timesteps are depicted from left to right. The time shown is relative to the first, whose absolute time is 1.221 Gyr. Five fields are displayed: (row 1) velocity (cm/yr), (row 2) temperature (K), (row 3) melt fraction, (row 4) basalt fraction, and (row 5) viscosity (Pa·s). In the top row, the velocity colorscale is cut to a maximum value of 2.53 cm/yr to make it possible to observe plates clearly.The white arrows on top of the domain show the surface velocity magnitude and direction. Three sequences of events are illustrated: (A1-4) Different plates exist, showing different surface velocities. In particular a small plate is visible in A1. A lithospheric delamination starts developing in A2, keeps developing and partly detaches in A4, leading to decoupling of the small plate with the plate to its left, and merging with the plate to its right (A3). (B1-4) A lithospheric delamination is underway in B1, keeps developing in B2 and eventually detaches in B4, leading to the disappearance of the previously existing plate boundary, as shown in B3. (C1-4) Due to return flow a portion of the upper mantle undergoes decompression melting (C1) leading to relatively high melt fractions (C4) and a high temperature anomaly (C3) in the lithosphere. These events create a new plate boundary, breaking the previously existing plate and forming a new independent plate (C2).

manuscript submitted to *Geochemistry, Geophysics, Geosystems*

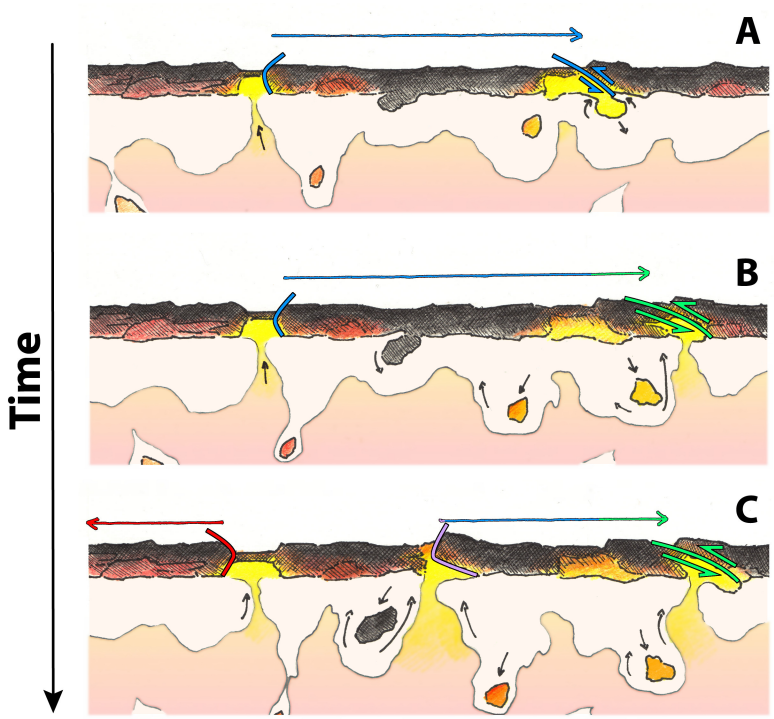

Figure 9: Illustration of the dynamics and evolution of a plutonic-squishy lid. The crust is depicted as the top layer in darker colours in each subplot. Below it, white material is warmer than the crust, which is in turn colder than the pink material underneath it. Yellow material is partially molten. Blue, green, purple and red lines show plate boundaries, while the arrows in the same colours represent extent and direction of selected plates.

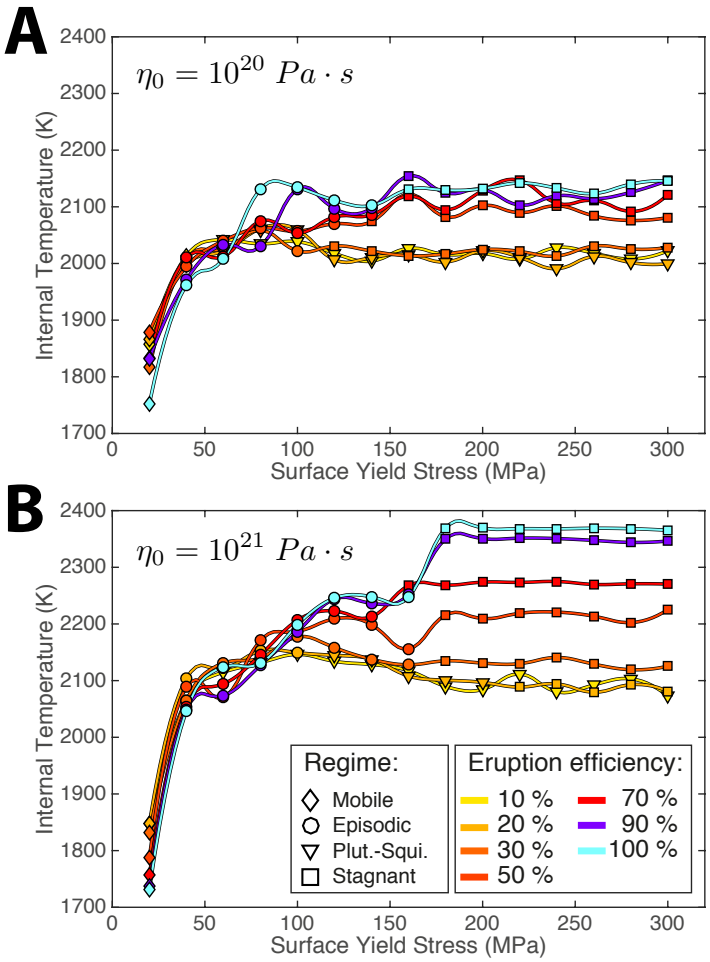

Figure 10: Asthenosphere temperature averaged over the last 500 Myr for each simulation. Different eruption efficiencies are represented by curves of different colours linking different symbols, which represent different tectonic regimes.The reference viscosity is: (A) 10^{20} Pa·s, and (B) 10^{21} Pa·s.

cantly depend on the eruption efficiency, showing coherence as a separate regime. Finally, in the stagnant-lid regime the internal temperature is only dependent on the eruption efficiency, which is an expected result since no mechanical (as opposed to magmatic) resurfacing ever occurs. We observe that in general the internal temperatures increase with increasing eruption efficiency. This result is explained next.

4.3 Heat flow

Fig. 11 depicts the magmatic (left panels) and conductive (right panels) heat flows averaged over the last 2 Gyr of evolution for each simulation. The magmatic heat flow is computed from the energy (i.e., latent heat of melt, and "thermal" heat) carried by the tracers that are extruded from the interior to the surface, as explained in Nakagawa and Tackley (2012). Intruded tracers do not contribute to this value since their heat is deposited at the bottom of the crust. The conductive heat flow is computed only from the heat diffusion at the top of the lithosphere, thereby excluding any heat flow carried by melt eruption.

In the mobile-lid regime, the magmatic heat flow is low. It increases by a few TW with increasing eruption rate. In the plutonic-squishy-lid regime, the magmatic heat flux is also low, and always increases by a small amount with both increasing yield stress and eruption rate, up to ∼10 TW. In cases with an episodic lid, the magmatic heat flow increases slightly (up to 20 TW) with increasing surface yield stress for the low reference viscosity cases. However, for the high reference viscosity cases, the magmatic heat flow decreases faintly with increasing surface yield stress values. Lastly, cases in the stagnant-lid regime show a strong increase in the magmatic heat flow with increasing eruption efficiency, with values as high as 30-35 TW.

To first order, the conductive heat flow follows an opposite trend compared to magmatic heat flow, since high eruption rates tend to thicken the top boundary layer, which results in lower conductive heat flows. The conductive heat flow is very high for cases in a mobile-lid regime, with values in the range of 35-45 TW. This value decreases with increasing eruption rate. In the episodic- and plutonic-squishy-lid regimes, the conductive heat flow is intermediate and diminishes with both increasing yield stress and eruption rate. This can be understood by the fact that the lithosphere has time to grow thicker in cases with rare resurfacing events. In the stagnant-lid regime, conductive heat fluxes are generally low, and systematically decrease with increasing eruption rate due to increasing lithospheric thicknesses.

Cases with a plutonic-squishy lid display relatively low magmatic heat fluxes because this regime only occurs for low extrusion efficiencies; however, they experience very high conductive heat flows compared to a planet covered with a stagnant lid. This makes this regime quite efficient at cooling a planet even if there is no on-going subduction or lithosphere overturns. This surprising result has been studied further in a recently published work by Lourenço et al. (2018), where it was found that warm intrusive magmatism acts to thin the lithosphere, leading to sustained recycling of overlying crustal material and efficient cooling of the mantle. In contrast, volcanic eruptions lead to a thick lithosphere that insulates the upper mantle and prevents efficient cooling. Moreover, it was found that high eruption efficiency depletes the mantle, which leads to the formation of little melt. Therefore, the mantle tends to warm up, whereas a re-fertilized mantle (due to high intrusion efficiency) can continuously melt and keep cooling down the mantle effectively. The results of the present work support the findings of Lourenço et al. (2018).

Finally, it is worth noting that the total surface heat flow (i.e. the sum of magmatic and conductive heat flows) for cases with a mobile lid obtained in our simulations are ∼ 40-50 TW. This provides support to our results as the average surface heat flow on Earth at present day is ∼ 44.4 TW (Turcotte & Schubert, 2014).

4.4 Distribution of basaltic material in the mantle and its effect on internal temperature and heat flow

Mantle temperatures and heat fluxes can only be understood by looking at the compositional state of the mantle, which has a critical effect on the solidus temperature. Fig. 1 portrays the final thermal and compositional state of a simulation in each of the tectonic regimes observed in this study. It shows that an enriched mantle (Fig. 1C) is more efficient at cooling the mantle than a depleted mantle (Fig. 1B and D) (cf. Bédard, 2006; Nakagawa & Tackley, 2015). Fig. 12 shows an overview of how basaltic material is distributed in the mantle by the end of the simulations performed in this study. We analyse this distribution by portraying three domains: (1) basaltic crust thickness, in Fig. 12(left), (2) mid-mantle-depth basalt fraction, in Fig. 12(center), and (3) basal layer thickness in Fig. 12(right), which represents the thermo-chemical piles formed near the core-mantle boundary (CMB) following subduction or any other process that brings lithospheric basaltic material into the deep mantle. Initially, the basalt fraction is 20% ev-

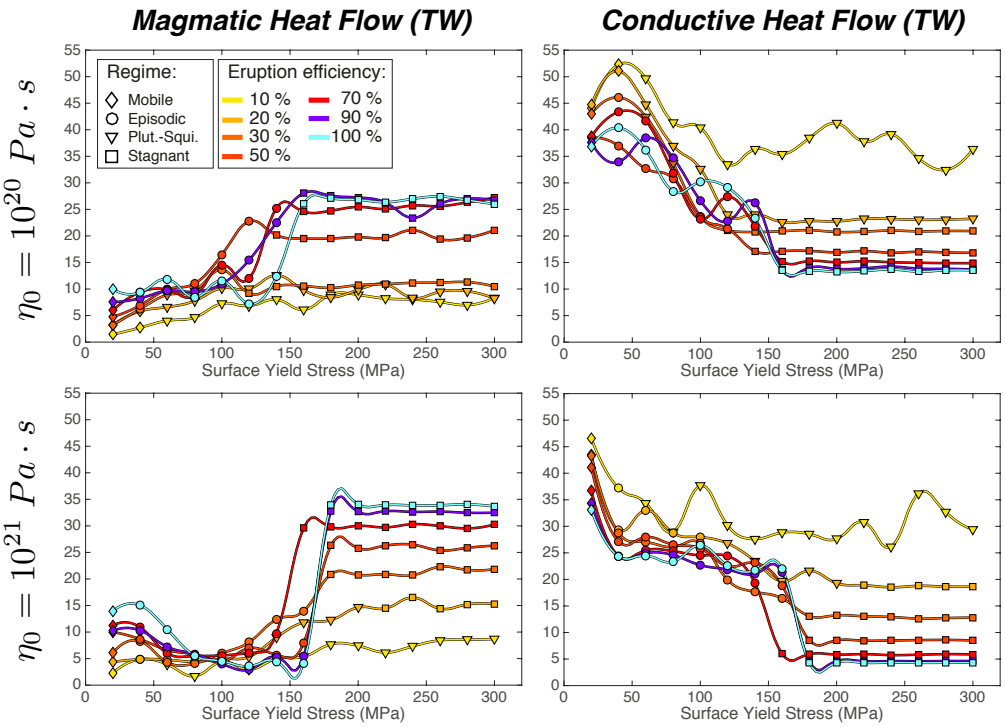

Figure 11: Magmatic (left) and conductive (right) heat flows, averaged over the last 2 Gyr for each simulation. In the top panels the reference viscosity $\eta_0 = 10^{20}$ Pa·s, while in the bottom panels $\eta_0 = 10^{21}$ Pa·s. Different eruption efficiencies are represented by curves of different colours linking different symbols, which represent different tectonic regimes.

561 erywhere. The top panels in Fig. 12 depict cases with a lower reference viscosity (10^{20}
562 $Pa \cdot s$), while the lower panels show cases with a higher reference viscosity (10^{21} $Pa \cdot$
563 s). All the values in Fig. 12 are averaged over the last 500 Myr of evolution of the planet.
564 An extended discussion about basal layer thicknesses obtained by different tectonic regimes,
565 and how do those thicknesses compare with seismically slow lower-mantle structures near
566 the Earth's CMB, the so-called large low shear velocity provinces (LLSVPs), is presented
567 in the Supplementary Material.

568 #### *4.4.1 Stagnant lid*

569 In cases with a stagnant lid, crustal thicknesses are large and strongly depend on
570 extrusion efficiency: intuitively, the higher the extrusion efficiency, the thicker becomes
571 the crust. Crustal thicknesses of hundreds of km can be obtained. Such amounts of crust
572 can only be stored because of the absence of both subduction and intrusive magmatism,
573 which acts to weaken the lithosphere. A higher eruption efficiency leads to a strong litho-
574 sphere and allows for such large crustal thicknesses, even if basalt turns into eclogite and
575 becomes denser (Lourenço et al., 2016). Cases with low eruption efficiency have thin-
576 ner crusts because plutonism eases eclogitic delaminations by warming up the crust.

577 When the eruption efficiency is large, for example 100% (Fig. 1D), the crust/lithosphere
578 becomes very thick (as previously observed by Armann and Tackley (2012)), which (1)
579 insulates the mantle from the surface, leading to low conductive heat flow (see Fig. 11,
580 bottom panels), and (2) strongly depletes the mantle through volcanic (heat) piping, which
581 therefore cannot efficiently melt and as a consequence also cannot cool down (melting
582 combined with magmatism is a very efficient heat loss mechanism (Xie & Tackley, 2004;
583 Ogawa & Yanagisawa, 2011; Nakagawa & Tackley, 2012)). This depletion mostly occurs
584 in the upper mantle but extends also into the mid- and lower mantle. In such cases, the
585 depleted mantle warms up the crust from the bottom, which leads to continuous crust
586 internal overturns. This explains why the magmatic heat flow for cases with a stagnant
587 lid and high reference viscosity is very large (Fig. 11, bottom left) without cooling the
588 mantle very efficiently.

589 In cases with lower viscosity (10^{20} $Pa \cdot s$) the crust cannot grow thicker than $\sim$
590 100 km (Fig. 12, top left), even if the eruption efficiency is 100%. This is an expected
591 behaviour as boundary layer thicknesses in a convecting fluid decrease with decreasing
592 viscosity (Fowler, 1985; Reese et al., 1998; Solomatov, 2004). Thinner crustal thicknesses
593 allow for a more efficient conductive cooling at the top (Fig. 11, top right) leading to
594 low internal temperatures. Because of this limitation on the crustal thickness for lower
595 reference viscosity cases, a substantial amount of eclogite is then recycled from the bot-
596 tom of the lithosphere into the deep mantle, which in turn generates a thick basal layer,
597 with values as high as 500 km around the CMB, that efficiently insulates the mantle from
598 the core. Contrarily, for cases with a high reference viscosity (10^{21} $Pa{\cdot}s$), independently
599 of the eruption efficiency, only a small amount of basalt is able to reach the basal layer,
600 as no subduction or lid delamination occurs. Basal layer thicknesses increase with in-
601 creasing eruption efficiency, but do not exceed $\sim$ 150 km when $\eta_0 = 10^{21}$ Pa·s.

602 #### *4.4.2 Episodic lid*

603 In the episodic-lid regime, and for both reference viscosities, the alternation of over-
604 turns and stagnant phases leads to mid-mantle basalt contents that are strongly vari-
605 able, systematically decreasing with increasing yield stress. At yield stresses around 100
606 MPa, the mantle is predicted to be almost completely depleted. The basaltic crust is re-
607 built during the stagnant phases (starting during the overturn itself), and may resur-
608 face again. Therefore, crustal thickness values strongly vary depending on the number
609 of overturn events. In general, crustal thicknesses increases with increasing yield stress,
610 as the number of overturns decreases. Furthermore, the closest in time to present-day

that an overturn event last happened, the thinner will be the crust as there is no time for a thick crust to form (again). Successive resurfacing events result in thick basal layers around the CMB (Armann & Tackley, 2012; Nakagawa & Tackley, 2015; Lourenço et al., 2016), as shown in Fig. 1B for a typical episodic lid case. The basal layer thickness strongly increases with increasing yield stress, up to 800 km. As can be seen in Fig. 4, two to four resurfacing events are needed in order to build such high thicknesses. This shows that rare but massive resurfacing events, which occur after significant crustal thicknesses have built up, are able to transport basaltic crustal material to the CMB more efficiently than frequent and small resurfacing events. Even if the number of overturns in the evolution of a planet is generally low, a lot of heat is released during them. This, combined with a thick basal layer insulating the core leads to lower internal temperatures compared to planets covered with a stagnant lid (Fig. 1B).

4.4.3 Mobile lid

Small crustal thicknesses are obtained for the cases in a mobile-lid regime, due to the efficient recycling of the lithosphere caused by continuous subduction, and lower internal temperatures due to efficient heat loss. The basalt content of the mid-mantle is always relatively high, indicating that basalt is efficiently (re)cycled into the lower mantle. This efficient mixing in the mantle leads to thin basal layers when compared to other tectonic regimes: $\sim$ 200 km for the higher reference viscosity (10^{21} Pa·s) and $\sim$ 400 km for the lower reference viscosity (10^{20} Pa·s).

4.4.4 Plutonic-squishy lid

In all cases in the plutonic-squishy-lid regime, due to high intrusion efficiencies, the lithosphere remains too warm to grow. Due to the thin lithosphere in this regime, conductive heat flow becomes very large (see Fig. 11, right panels). Crustal thicknesses increase with increasing yield stress until a plateau value of 50 to 100 km is reached. Hot eclogite constantly drips into the convecting mantle from the bottom of the crust. Part of it is entrained in the mantle circulation keeping the internal ambient mantle enriched, whereas the other part settles and forms a thick basal layer at the CMB. Basal layer thicknesses are high, similarly to what occurs in the episodic-lid regime. These large basal layer thicknesses show that eclogite drips coming from the bottom of the lithosphere are not only re-stirred into the mantle but are also efficiently deposited near the CMB in the plutonic-squishy-lid regime. A thick basal layer in addition to large surface heat flow, are responsible for the significantly low internal temperatures (Fig. 1C).

5 Plutonic-squishy-lid regime: implications, possible applications, and future work

The main finding of this work is the new plutonic-squishy-lid regime. In this section we discuss implications and possible applications of this regime to the Archean Earth and Venus, and how it can help understanding some of the most important unanswered questions about the evolution of the Earth.

5.1 Archean Earth

An outstanding unresolved question about the evolution of the Earth is what was the tectonic regime active before the onset of plate tectonics. van Hunen and van den Berg (2008) focused on the effects that a hotter mantle would have on subduction and found that an increase of 200-300 K in the mantle potential temperature leads to episodic subduction due to frequent slab break-off. Further work by Sizova et al. (2010) and Fischer and Gerya (2016a, 2016b) identified several geodynamic regimes depending on the mantle potential temperature (T_p) using 2-D and 3-D regional numerical models, respectively.

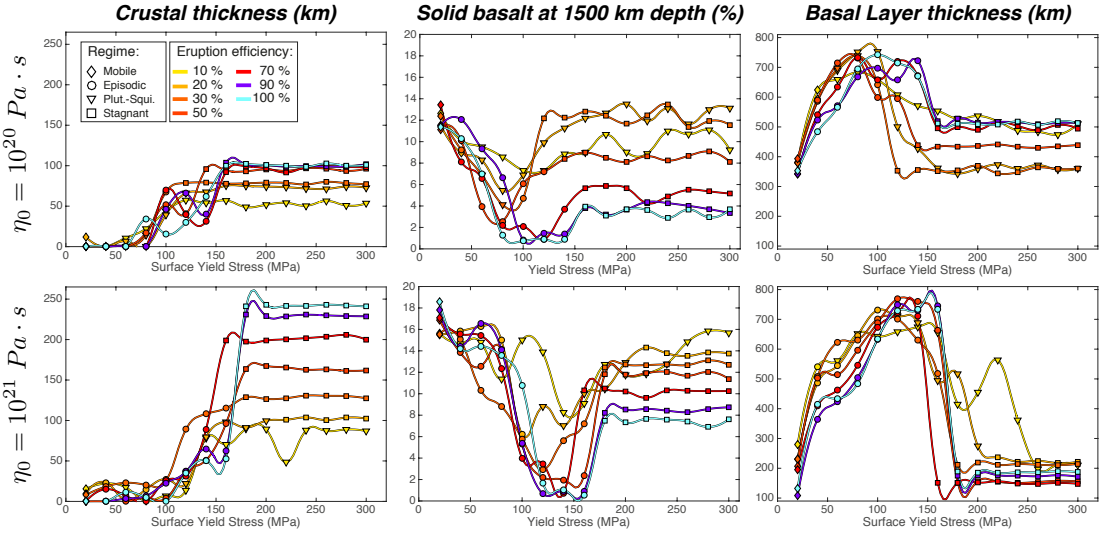

Figure 12: Crustal thickness (left), internal composition represented by the solid basalt fraction at 1500 km depth (middle) and basal layer thickness (right), averaged over the last 500 Myr for each simulation. In the top panels the reference viscosity $\eta_0 = 10^{20}$ Pa·s, while in the bottom panels $\eta_0 = 10^{21}$ Pa·s. Different eruption efficiencies are represented by curves of different colours linking different symbols, which represent different tectonic regimes.

These papers explored how the styles of subduction could have changed throughout the Precambrian until the present day by assigning to the model different T_p values, corresponding to different times in the evolution of the Earth. As the T_p is decreased, regimes range from a so-called plume-lid regime, to a regime of dripping subduction, characterised by frequent dripping from the slab tip and a loss of coherence of the slab, to modern-day plate tectonics. The plume-lid regime would have been active in the Archean and was dominated by widespread development of lithospheric delamination and eclogitic drips, a weak and highly heterogeneous lithosphere, and small plates. The present work presents new evidence for a new global tectonic regime, with similarities to the plume-lid regime described by Sizova et al. (2010) and Fischer and Gerya (2016a, 2016b). This new regime, which we name plutonic-squishy lid is active for high mantle temperatures and high intrusion efficiencies, the conditions of the early Earth. It is dominated by extensive development of lithospheric delamination and eclogitic drips, and a lithosphere divided into plates separated by deformable and weak plate boundaries due to plutonism. Our model differs from the plume-lid one in the fact that, whereas our model shows high plateness, the plume-lid regime is characterised by a weak internally-convecting crust.

Explanations of the geological record older than 3 Gyr are generally divided into: (1) (proto)plate tectonic models, which would feature modern-day-like characteristics such as horizontal plate motion, with spreading ridges and subduction zones (Harrison, 2009), and (2) vertical tectonic models, characterized by lithospheric diapirism, associated downwelling and volcanism, and basal delamination (van Thienen, Vlaar, & van den Berg, 2005; Stern, 2008; Moore & Webb, 2013). Both these models present advantages and disadvantages. The plate tectonics models are supported by detrital zircons coming from Jack Hills, Western Australia, which suggest that an ocean might have been present 4.4 billions of years ago, giving the lithosphere a sufficient rigidity for plate tectonics to operate (Watson & Harrison, 2005). However, the presence of water, even if a necessary precondition for plate tectonics, does not necessarily imply that a plate-tectonics

regime was operating. The isotopic systematics of the Jack Hills zircons resembles modern Earth convergent margin settings, again suggesting the operation of plate tectonics (Harrison et al., 2005). Yet, even if the geochemical signatures of the Jack Hills zircons can be linked to subduction magmas (cf. Bédard, Harris, & Thurston, 2013), the existence of convergent margins does not necessarily mean plate tectonics, as can be inferred, for example, by the existence of the ~ 1000 km wide orogen formed ahead of the drifting Lakhmi planum on Venus (Harris & Bédard, 2015; Bédard, 2018). These (proto)plate tectonic models cannot explain the absence of plate tectonics products, some of them with high preservation potential, such as paired metamorphic belts and passive margins (Stern, 2008). The opposite happens for vertical tectonics models: they can explain the lack of plate tectonics evidence but they cannot explain horizontal motion. Moore and Webb (2013), who propose a vertical heat-pipe regime for the Archean Earth, argue that the horizontal motion comes from lateral-compression as rocks are forced radially inward due to volcanic material deposited at the surface, however the magnitude of this horizontal motion is not quantified.

Bédard (2018) proposed a model based on geological and geochemical evidence that aims at bridging horizontal and vertical tectonic models. A periodically destabilized stagnant lid regime (or episodic lid as defined in this study) is proposed. Vertical motion is generated by mantle overturns that lead to the destabilization of the lid, while horizontal motion is driven by mantle currents pressing against continental blocks with deep lithospheric keels. This implies that a continental drift system began in the Early Archean, while modern-style active subduction is proposed to have started near the end of the Archean, around 2.5 Ga. The model we present in this work, the plutonic-squishy-lid model, also has the potential of bridging horizontal and vertical models: it shows horizontal plate motion, together with vertical diapirism, volcanism, delaminations and drippings. These features lead to high surface heat flux, which is thought to be the case in the Archean (Lenardic, 2013). The plutonic-squishy-lid regime also exhibits the components needed to the formation of continental crust, i.e. delamination of the lower eclogitic part of an oceanic protocrust, which would lead to the production of tonalite, trondhjemite, and granodiorite (TTG) suites (Rozel, Golabek, Jain, Tackley, & Gerya, 2017; Jain, Rozel, Tackley, Sanan, & Gerya, 2019) as recorded in Archean cratons (Martin, 1987; Zegers & van Keken, 2001; Moyen & Martin, 2012; Johnson et al., 2014). Due to these reasons, the plutonic-squishy-lid regime seems to be a prime candidate to have been active during the Archean Earth, and future work should investigate this possibility further.

5.2 Venus

Another potential application of the plutonic-squishy-lid regime might be Venus. Venus has a strikingly homogeneous meteoritic cratering surface record (Strom, Schaber, & Dawson, 1994). The exact mechanisms that lead to this are debated but the process was presumably resurfacing, Venus being in an episodic-lid regime (Turcotte, 1993; Moresi & Solomatov, 1998; Noack et al., 2012; Rozel, 2012; Armann & Tackley, 2012). However, significant lateral motions of continental-like domains can be observed (Harris & Bédard, 2015), and surface deformation strain rates of $10^{-17} - 10^{-18}$ /s have been inferred for recent history, though this value can go up to 10^{-15} /s in the past (Grimm, 1994). Furthermore, there is widespread evidence of interactions of plumes with the lithosphere: examples include 513 corona and 64 nova (Stofan, Smrekar, Tapper, Guest, & Grindrod, 2001; Glaze, Stofan, Smrekar, & Baloga, 2002; Krassilnikov & Head, 2003; Gerya, 2014). All these features point to significant lid mobility without subduction. It is also important to note that Venus' lithosphere is expected to be warm and soft due to high surface temperature (Gerya, 2014). Therefore, the plutonic-squishy-lid regime we describe in this work might be applicable for Venus, and further work should strive to investigate this possibility.

5.3 Future work

A second outstanding question that remains unanswered about the evolution of the Earth is when did plate tectonics initiate (e.g., Korenaga, 2013; Harris & Bédard, 2015; Condie, 2016; Bédard, 2018). Understanding the tectonic evolution of the Earth can help to solve other outstanding questions still standing, for example, knowing when plate tectonics started can help to add constraints on important related topics including the long-term geological carbon-cycle (Walker, Hays, & Kasting, 1981) and deep water cycle (van Keken, Hacker, Syracuse, & Abers, 2011). The present work can have implications for possible previously active tectonic regimes on Earth, however it does not give a clear answer on the time evolution and transitions between them. Some of our simulations display time-dependency ("maturation") of a given tectonic regime as the planet evolves. For example, it is common that in an episodic-lid regime the number and intensity of overturns decrease with time. Also, for high intrusion efficiencies, the mobile-lid regime displays some time-dependency, evolving from a more dripping state, where oceanic lithosphere sinking is relatively short-lived, to a more smoothly and long-lasting subduction, as the planet cools down. However, our models rarely portray transitions between different regimes in the evolution of an individual case. We note, however, that we assume here that the effective lithospheric yield stress, a parametric value that summarizes physical processes on the micro scales that are relevant for plastic deformation, is constant. Future work is needed to enhance this parameterization, or even directly model more realistic physics, such as damage due to grain size evolution (Bercovici & Ricard, 2005; Ricard & Bercovici, 2009; Rozel, Ricard, & Bercovici, 2011; Bercovici & Ricard, 2014) or magmatic weakening (Sizova et al., 2010; Gerya et al., 2015). Modelling the formation of TTGs and continental crust (due to remelting of oceanic crust under certain conditions) should also be an aim of future work as the presence of these should affect the dynamics and evolution of the lithosphere (Jain et al., 2019). A related complexity will be the study of the effect of magma emplacement at mid-crustal depths, between the predominantly felsic continental upper crust and the more mafic continental lower crust, and thought to be important for the case of continental crust (e.g., Sparks, Meyer, & Sigurdsson, 1980). Test cases elucidate that the plutonic-squishy lid regime is promoted by intrusions placed at mid-crustal depths (as opposed to the base of the crust), particularly for high-resolution cases.

Finally, future 3D studies are needed to characterize in detail the plutonic-squishy-lid regime, in particular (1) how localized intrusions will connect to each other to form more diffuse plate boundaries, (2) the behaviour of lithospheric drips, in particular how these drips may resemble in many ways subduction zones with regular slab break-off because plastic deformation is strongly involved in the process (e.g., van Hunen & van den Berg, 2008), and (3) plate size, distribution, and associated surface motion and deformation.

6 Conclusions

In this work we investigate the impact of intrusive magmatism efficiency, surface yield stress and reference viscosity on the tectonic regimes of Earth-like planets, through a set of numerical simulations of thermo-chemical mantle convection. Four tectonic/convective regimes are obtained. Three of them have been observed before: (1) a mobile-lid regime (plate tectonics) always exits at low yield stress, (2) an episodic-lid regime is active for intermediate yield stress values and intermediate to high eruption efficiencies, (3) a stagnant-lid regime exists for large yield stress values and high eruption efficiency. The fourth tectonic regime obtained, the plutonic-squishy-lid regime, is newly described in this study and exists for high intrusion efficiencies ($\geq 70\%$). This regime is characterized by the existence of small, strong, ephemeral plates separated by warm and weak regions generated by plutonism. Warm eclogitic drips and lithosperic delaminations are common and lead to: (1) significant surface velocities even if subduction is not active, (2) con-

tinuous mixing of the bottom of the lithosphere into the convecting mantle, and (3) a thin lithosphere, which results in high conductive heat fluxes and relatively low internal mantle temperatures. This tectonic regime can have implications for Venus and the early Earth, as it is able to combine features of both horizontal and vertical tectonics models. A general conclusion of the present study is that the evolution and internal state of a planet are not only conditioned by its rheology and boundary conditions, but also depend strongly on plutonic and eruptive processes associated with melting, and the relative importance of them.

Acknowledgments

D.L.L. was supported by ETH Zurich grant ETH-46 12-1. A.R. received funding from the European Research Council under the European Union's Seventh Framework Programme (FP/2007-2013) / ERC Grant Agreement n. 320639 project iGEO. The simulation data and scripts used to treat it that lead to the results present in this study will be uploaded to the repository Zenodo (https://zenodo.org/) by acceptance. The convection code StagYY is the property of P.J.T. and ETH Zurich, and is available for collaborative studies from P.J.T. (paul.tackley@erdw.ethz.ch). The authors thank Taras Gerya and Adina Pusok for very helpful discussions.

References

Abe, Y. (1993). Thermal evolution and chemical differentiation of the terrestrial magma ocean. In *Evolution of the earth and planets* (pp. 41–54). Washington, D. C.: American Geophysical Union.

Abe, Y. (1997). Thermal and chemical evolution of the terrestrial magma ocean. *Physics of the Earth and Planetary Interiors*, *100*, 27–39.

Armann, M., & Tackley, P. (2012). Simulating the thermochemical magmatic and tectonic evolution of Venus's mantle and lithosphere: Two-dimensional models. *J. Geophys. Res.*, *117*(E12003). doi: 10.1029/2012JE004231

Arzi, A. A. (1978). Critical phenomena in the rheology of partially melted rocks. *Tectonophysics*, *44*, 173–184.

Balay, S., Brown, J., Buschelman, K., Eijkhout, V., W. Gropp, D. K., Knepley, M., ... Zhang, H. (2012). Petsc users manual, anl-95/11 –revision 3.3 [Computer software manual].

Bédard, J. H. (2006). A catalytic delamination-driven model for coupled genesis of Archaean crust and sub-continental lithospheric mantle. *Geochimica Et Cosmochimica Acta*, *70*(5), 1188–1214.

Bédard, J. H., Harris, L. B., & Thurston, P. C. (2013). The hunting of the snarc. *Precambrian Research*, *229*, 20 - 48. Retrieved from `http://www.sciencedirect.com/science/article/pii/S0301926812000897` (Evolving Early Earth) doi: http://dx.doi.org/10.1016/j.precamres.2012.04.001

Bercovici, D., & Ricard, Y. (2005, March). Tectonic plate generation and two-phase damage: Void growth versus grain size reduction. *Journal of Geophysical Research: Solid Earth (1978–2012)*, *110*(B3).

Bercovici, D., & Ricard, Y. (2014, April). Plate tectonics, damage and inheritance. *Nature*, *508*(7497), 513–516.

Buffett, B. A., Huppert, H. E., Lister, J. R., & Woods, A. W. (1992, March). Analytical model for solidification of the Earth's core. *Nature*, *356*(6367), 329–331.

Buffett, B. A., Huppert, H. E., Lister, J. R., & Woods, A. W. (1996). On the thermal evolution of the Earth's core. *Journal of Geophysical Research*, *101*(B4), 7989–8006.

Bédard, J. H. (2018). Stagnant lids and mantle overturns: Implications for archaean tectonics, magmagenesis, crustal growth, mantle evolution, and the

start of plate tectonics. *Geoscience Frontiers*, *9*(1), 19 - 49. Retrieved from http://www.sciencedirect.com/science/article/pii/S1674987117300233 (Lid Tectonics) doi: https://doi.org/10.1016/j.gsf.2017.01.005

Cawood, P. A., Hawkesworth, C. J., & Dhuime, B. (2013). The continental record and the generation of continental crust. *Geological Society of America Bulletin*, *125*(1-2), 14–32.

Christensen, U. R. (1984, November). Heat transport by variable viscosity convection and implications for the Earth's thermal evolution. *Physics of the Earth and Planetary Interiors*, *35*(4), 264–282.

Condie, K. C. (2016). A planet in transition: The onset of plate tectonics on earth between 3 and 2 ga? *Geoscience Frontiers*. Retrieved from http://www.sciencedirect.com/science/article/pii/S167498711630127X doi: http://dx.doi.org/10.1016/j.gsf.2016.09.001

Condomines, M., Hemond, C., & Allègre, C. J. (1988). U-th-ra radioactive disequilibria and magmatic processes. *Earth and Planetary Science Letters*, *90*(3), 243–262.

Costa, A., Caricchi, L., & Bagdassarov, N. (2009). A model for the rheology of particle-bearing suspensions and partially molten rocks. *Geochemistry, Geophysics, Geosystems*, *10*(3).

Crisp, J. A. (1984). Rates of magma emplacement and volcanic output. *Journal of Volcanology and Geothermal Research*, *20*(3-4), 177–211.

Davies, G. F. (1995). Punctuated tectonic evolution of the earth. *Earth and Planetary Science Letters*, *136*(3), 363 - 379. Retrieved from http://www.sciencedirect.com/science/article/pii/0012821X9500167B doi: https://doi.org/10.1016/0012-821X(95)00167-B

Dymkova, D., & Gerya, T. (2013). Porous fluid flow enables oceanic subduction initiation on earth. *Geophys. Res. Lett.*, *40*, 5671–5676. doi: 10.1002/2013GL057798

Fischer, R., & Gerya, T. (2016a). Early earth plume-lid tectonics: A high-resolution 3d numerical modelling approach. *Journal of Geodynamics*. doi: http://dx.doi.org/doi:10.1016/j.jog.2016.03.004

Fischer, R., & Gerya, T. (2016b, September). Regimes of subduction and lithospheric dynamics in the Precambrian: 3D thermomechanical modelling. *Gondwana Research*, *37*, 53–70.

Foley, B., & Bercovici, D. (2014). Scaling laws for convection with temperature-dependent viscosity and grain-damage. *Geophys. Journ. Int.*, *199*(1), 580–603.

Fowler, A. C. (1985). Fast thermoviscous convection. *Stud. appl. math.*, *72*, 189–219.

Fowler, A. C. (1993). Boundary layer theory and subduction. *Journ. Geophys. Res.*, *98*(B12), 21997–22005.

Gerya, T. V. (2014). Plume-induced crustal convection: 3D thermomechanical model and implications for the origin of novae and coronae on Venus. *Earth and Planetary Science Letters*, *391*, 183–192.

Gerya, T. V., Stern, R. J., Baes, M., Sobolev, S. V., & Whattam, S. A. (2015). Plate tectonics on the Earth triggered by plume-induced subduction initiation. *Nature*, *527*(7577), 221–225.

Glaze, L. S., Stofan, E. R., Smrekar, S. E., & Baloga, S. M. (2002). Insights into corona formation through statistical analyses. *Journal of Geophysical Research: Planets*, *107*(E12).

Gordon, R. G., & Stein, S. (1992). Global Tectonics and Space Geodesy. *Science*, *256*(5055), 333–342.

Grimm, R. E. (1994). Recent Deformation Rates on Venus. *Journal of Geophysical Research: Planets*, *99*(E11), 23163–23171.

Harris, L. B., & Bédard, J. H. (2015, January). Interactions between continent-like 'drift', rifting and mantle flow on Venus: gravity interpretations and Earth

analogues. *Geological Society, London, Special Publications*, *401*(1), 327–356.
Harrison, T. M. (2009). The hadean crust: Evidence from >4 ga zircons. *Annual Review of Earth and Planetary Sciences*, *37*(1), 479-505. Retrieved from http://dx.doi.org/10.1146/annurev.earth.031208.100151 doi: 10.1146/annurev.earth.031208.100151
Harrison, T. M., Blichert-Toft, J., Müller, W., Albarede, F., Holden, P., & Mojzsis, S. J. (2005). Heterogeneous hadean hafnium: Evidence of continental crust at 4.4 to 4.5 ga. *Science*, *310*(5756), 1947–1950. Retrieved from http://science.sciencemag.org/content/310/5756/1947 doi: 10.1126/science.1117926
Hernlund, J. W., & Tackley, P. J. (2008). Modeling mantle convection in the spherical annulus. *Phys. Earth Plan. Int.*, *171*(1-4), 48 - 54. doi: 10.1016/j.pepi.2008.07.037
Herzberg, C., Condie, C., & Korenaga, J. (2010). Thermal history of the earth and its petrological expression. *Earth Planet. Sci. Lett.*, *292*, 79–88.
Herzberg, C., Raterron, P., & Zhang, J. (2000, November). New experimental observations on the anhydrous solidus for peridotite KLB-1. *Geochemistry, Geophysics, Geosystems*, *1*(11).
Hirth, G., & Kohlstedt, D. (2003). Rheology of the upper mantle and the mantle wedge: a view from the experimentalists. In J. Eiler (Ed.), *Subduction factory monograph* (Vol. 138, p. 83-105). Washington, DC: Am. Geophys. Union.
Irifune, T., & Ringwood, A. (1993). Phase transformations in subducted oceanic crust and buoyancy relationships at depths of 600-800 km in the mantle. *Earth and Planet. Sci. Lett.*, *117*(1–2), 101–110.
Jain, C., Rozel, A. B., Tackley, P. J., Sanan, P., & Gerya, T. V. (2019). Growing primordial continental crust self-consistently in global mantle convection models. *Gondwana Research*, *73*, 96 - 122. Retrieved from http://www.sciencedirect.com/science/article/pii/S1342937X19301066 doi: https://doi.org/10.1016/j.gr.2019.03.015
Jaupart, C., Labrosse, S., & Mareschal, J.-C. (2007). Temperatures, heat and energy in the mantle of the earth. In G. Schubert (Ed.), *Treatise on geophysics* (p. 253 - 303). Amsterdam: Elsevier. doi: DOI:10.1016/B978-044452748-6.00114-0
Johnson, T. E., Brown, M., Kaus, B. J. P., & VanTongeren, J. A. (2014, January). Delamination and recycling of Archaean crust caused by gravitational instabilities. *Nature Geoscience*, *7*(1), 47–52.
Karato, S.-I., & Wu, P. (1993). Rheology of the upper mantle: A synthesis. *Science*, *260*(5109), 771–778.
Kohlstedt, D., Evans, B., & Mackwell, S. (1995). Strength of the lithosphere: constraints imposed by laboratory experiments. *J. Geophys. Res.*, *100*, 17587–17602.
Korenaga, J. (2013). Initiation and evolution of plate tectonics on earth: Theories and observations. *Annual Review of Earth and Planetary Sciences*, *41*(1), 117-151. Retrieved from http://dx.doi.org/10.1146/annurev-earth-050212-124208 doi: 10.1146/annurev-earth-050212-124208
Krassilnikov, A. S., & Head, J. W. (2003). Novae on Venus: Geology, classification, and evolution. *Journal of Geophysical Research: Planets*, *108*(E9).
Lenardic, A. (2013). Continental growth and the archean paradox. In *Archean geodynamics and environments* (pp. 33–45). American Geophysical Union. Retrieved from http://dx.doi.org/10.1029/164GM04 doi: 10.1029/164GM04
Lourenço, D., Rozel, A., & Tackley, P. (2016). Melting-induced crustal production helps plate tectonics on earth-like planets. *Earth and Planetary Science Letters*, *438*, 18–28. doi: 10.1016/j.epsl.2016.01.024
Lourenço, D. L., Rozel, A. B., Gerya, T., & Tackley, P. J. (2018, May). Efficient cooling of rocky planets by intrusive magmatism. *Nature Geoscience*, *11*(5),

322–327.

Martin, H. (1987, October). Petrogenesis of Archaean Trondhjemites, Tonalites, and Granodiorites from Eastern Finland: Major and Trace Element Geochemistry. *Journal of Petrology*, *28*(5), 921–953.

Moore, W. B., & Webb, A. A. G. (2013, September). Heat-pipe Earth. *Nature*, *501*(7468), 501–505.

Moresi, L., & Solomatov, V. (1998). Mantle convection with a brittle lithosphere: Thoughts on the global tectonic style of the Earth and Venus. *Geophys. J.*, *133*, 669–682.

Moyen, J.-F., & Laurent, O. (2018). Archaean tectonic systems: A view from igneous rocks. *Lithos*, *302-303*, 99 - 125. Retrieved from `http://www.sciencedirect.com/science/article/pii/S0024493717304292` doi: https://doi.org/10.1016/j.lithos.2017.11.038

Moyen, J.-F., & Martin, H. (2012). Forty years of TTG research. *Lithos*, *148*, 312–336.

Nakagawa, T., & Tackley, P. (2004). Thermo-chemical structure in the mantle arising from a three-component convective system and implications for geochemistry. *Physics of The Earth and Planetary Interiors*, *146*(1-2), 125 - 138. Retrieved from `http://www.sciencedirect.com/science/article/B6V6S-4C7DDX0-3/2/92affb5a8bc926c829b88aab89b564cc` (Plumes and Superplumes) doi: 10.1016/j.pepi.2003.05.006

Nakagawa, T., & Tackley, P. (2012). Influence of magmatism on mantle cooling, surface heat flow and urey ratio. *Earth and Planetary Science Letters*, *329-330*, 1–10. doi: 10.1016/j.epsl.2012.02.011

Nakagawa, T., & Tackley, P. J. (2015, October). Influence of plate tectonic mode on the coupled thermochemical evolution of Earth's mantle and core. *Geochemistry, Geophysics, Geosystems*, *16*(10), 3400–3413.

Nakagawa, T., Tackley, P. J., Deschamps, F., & Connolly, J. A. D. (2010, August). The influence of MORB and harzburgite composition on thermo-chemical mantle convection in a 3-D spherical shell with self-consistently calculated mineral physics. *Earth and Planetary Science Letters*, *296*(3-4), 403–412.

Nataf, H. C., & Richter, F. M. (1982, September). Convection experiments in fluids with highly temperature-dependent viscosity and the thermal evolution of the planets. *Physics of the Earth and Planetary Interiors*, *29*(3-4), 320–329.

Noack, L., Breuer, D., & Spohn, T. (2012). Coupling the atmosphere with interior dynamics: Implications for the resurfacing of Venus. *Icarus*, *217*(2), 484–498.

Ogawa, M., & Yanagisawa, T. (2011, August). Numerical models of Martian mantle evolution induced by magmatism and solid-state convection beneath stagnant lithosphere. *J. Geophys. Res.*, *116*(E8), E08008.

O'Neill, C., Jellinek, A. M., & Lenardic, A. (2007, September). Conditions for the onset of plate tectonics on terrestrial planets and moons. *Earth and Planetary Science Letters*, *261*(1-2), 20–32.

Ono, S., Ito, E., & Katsura, T. (2001). Mineralogy of subducted basaltic crust (morb) from 25 to 37 gpa, and chemical heterogeneity of the lower mantle. *Earth Planet. Sci. Lett.*, *190*(1–2), 57–63.

O'Reilly, T. C., & Davies, G. F. (1981). Magma transport of heat on io: A mechanism allowing a thick lithosphere. *Geophys. Res. Lett.*, *8*, 313-316.

O'Rourke, J. G., Wolf, A. S., & Ehlmann, B. L. (2014). Venus: Interpreting the spatial distribution of volcanically modified craters. *Geophysical Research Letters*, 2014GL062121. doi: 10.1002/2014GL062121

Reese, C. C., Solomatov, V. S., & Moresi, L.-N. (1998). Heat transport efficiency for stagnant lid convection with dislocation viscosity: Application to Mars and Venus. *Journ. Geophys. Res.*, *103*, 13643–13657.

Regenauer-lieb, K., Yuen, D., & Branlund, J. (2001). The initiation of subduction: criticality by addition of water? *Science*, *294*(5542), 578–580.

Ricard, Y., & Bercovici, D. (2009). A continuum theory of grain size evolution and damage. *J. Geophys. Res.*, *114*, B01204.1-B01204.30.

Rolf, T., & Tackley, P. (2011). Focussing of stress by continents in 3D spherical mantle convection with self-consistent plate tectonics. *Geophys. Res. Lett.*, *38*(L18301). doi: 10.1029/2011GL048677

Rozel, A. (2012). Impact of grain size on the convection of terrestrial planets. *Geochem. Geophys. Geosyst.*, *13*(Q10020). doi: 10.1029/2012GC004282

Rozel, A., Golabek, G., Naef, R., & Tackley, P. (2015). Formation of ridges in a stable lithosphere in mantle convection models with a viscoplastic rheology. *Geophys. Res. Lett.*, *42*, 4770–4777. doi: 10.1002/2015GL063483

Rozel, A., Golabek, G. J., Jain, C., Tackley, P. J., & Gerya, T. (2017, May). Continental crust formation on early Earth controlled by intrusive magmatism. *Nature*, *545*(7654), 332–335.

Rozel, A., Ricard, Y., & Bercovici, D. (2011, February). A thermodynamically self-consistent damage equation for grain size evolution during dynamic recrystallization. *Geophysical Journal International*, *184*(2), 719–728.

Schubert, G., Turcotte, D., & Olson, P. (2001). *Mantle convection in the earth and planets*. Cambridge: Cambridge University Press.

Sizova, E., Gerya, T., Brown, M., & Perchuk, L. L. (2010, May). Subduction styles in the Precambrian: Insight from numerical experiments. *Lithos*, *116*(3-4), 209–229.

Sizova, E., Gerya, T., Stuwe, K., & Brown, M. (2015). Generation of felsic crust in the archean: A geodynamic modeling perspective. *Precambrian Research*, *271*, 198–224. doi: http://dx.doi.org/10.1016/j.precamres.2015.10.005

Solomatov, V. S. (1995). Scaling of temperature- and stress-dependent viscosity convection. *Phys. Fluids*, *7*, 266–274.

Solomatov, V. S. (2004). Initiation of subduction by small-scale convection. *Journ. Geophys. Res.*, *109*, B01412.

Sparks, R. S. J., Meyer, P., & Sigurdsson, H. (1980). Density Variation Amongst Mid-Ocean Ridge Basalts - Implications for Magma Mixing and the Scarcity of Primitive Lavas. *Earth and Planetary Science Letters*, *46*(3), 419–430.

Stein, C., Schmalzl, J., & Hansen, U. (2004). The effect of rheological parameters on plate behaviour in a self-consistent model of mantle convection. *Phys. Earth. Plan. Int.*, *142*, 225–255.

Stern, R. J. (2008, July). Modern-style plate tectonics began in Neoproterozoic time: An alternative interpretation of Earth's tectonic history. *Geological Society of America Special Papers*, *440*, 265–280.

Stofan, E. R., Smrekar, S. E., Tapper, S. W., Guest, J. E., & Grindrod, P. M. (2001). Preliminary analysis of an expanded corona database for Venus. *Geophysical Research Letters*, *28*(22), 4267–4270.

Strom, R. G., Schaber, G. G., & Dawson, D. D. (1994, May). The global resurfacing of Venus. *Journal of Geophysical Research: Planets*, *99*(E5), 10899–10926.

Sun, S. s., & McDonough, W. F. (1989). Chemical and isotopic systematics of oceanic basalts: implications for mantle composition and processes. *Geological Society, London, Special Publications*, *42*(1), 313–345.

Tackley, P. J. (2000). Self consistent generation of tectonic plates in time-dependent, three dimensional mantle convection simulations, part 1: Pseudoplastic yielding. *G3*, *1*(2000GC000036).

Tackley, P. J. (2008). Modelling compressible mantle convection with large viscosity contrasts in a three-dimensional spherical shell using the yin-yang grid. *Phys. Earth Plan. Int.*, *171*(1-4), 7 - 18. doi: 10.1016/j.pepi.2008.08.005

Turcotte, D. L. (1993, September). An episodic hypothesis for Venusian tectonics. *Journal of Geophysical Research: Planets (1991–2012)*, *98*(E9), 17061–17068.

Turcotte, D. L., & Schubert, G. (2014). *Geodynamics*. Cambridge University Press.

Valencia, D., & O'Connell, R. (2009). Convection scaling and subduction on earth and super-earths. *Earth and Plan. Sci. Lett.*, *286*, 492–502.

van Heck, H., & Tackley, P. (2011). Plate tectonics on super-Earths: Equally or more likely than on Earth. *Earth Planet. Sci. Lett.*, *310*, 252–261.

van Hunen, J., & van den Berg, A. P. (2008, June). Plate tectonics on the early Earth: Limitations imposed by strength and buoyancy of subducted lithosphere. *Lithos*, *103*(1-2), 217–235.

van Keken, P. E., Hacker, B. R., Syracuse, E. M., & Abers, G. A. (2011, January). Subduction factory: 4. Depth-dependent flux of H2O from subducting slabs worldwide. *Journal of Geophysical Research: Planets*, *116*(B1), B01401.

van Thienen, P., van den Berg, A., & Vlaar, N. (2004a). On the formation of continental silicic melts in thermochemical mantle convection models: implications for early earth. *Tectonophysics*, *394*(1), 111 - 124. Retrieved from `http://www.sciencedirect.com/science/article/pii/S004019510400304X` doi: https://doi.org/10.1016/j.tecto.2004.07.058

van Thienen, P., van den Berg, A., & Vlaar, N. (2004b). Production and recycling of oceanic crust in the early earth. *Tectonophysics*, *386*(1), 41 - 65. Retrieved from `http://www.sciencedirect.com/science/article/pii/S0040195104001544` doi: https://doi.org/10.1016/j.tecto.2004.04.027

van Thienen, P., Vlaar, N., & van den Berg, A. (2005). Assessment of the cooling capacity of plate tectonics and flood volcanism in the evolution of earth, mars and venus. *Physics of the Earth and Planetary Interiors*, *150*(4), 287 - 315. Retrieved from `http://www.sciencedirect.com/science/article/pii/S0031920104004030` doi: https://doi.org/10.1016/j.pepi.2004.11.010

Vogt, K., Gerya, T. V., & Castro, A. (2012, February). Crustal growth at active continental margins: Numerical modeling. *Physics of the Earth and Planetary Interiors*, *192*, 1–20.

Walker, J. C. G., Hays, P. B., & Kasting, J. F. (1981, October). A negative feedback mechanism for the long-term stabilization of Earth's surface temperature. *Journal of Geophysical Research: Planets*, *86*(C10), 9776–9782.

Watson, E. B., & Harrison, T. M. (2005). Zircon thermometer reveals minimum melting conditions on earliest earth. *Science*, *308*(5723), 841–844. Retrieved from `http://science.sciencemag.org/content/308/5723/841` doi: 10.1126/science.1110873

Weinstein, S. A., & Olson, P. L. (1992). Thermal convection with non-newtonian plates. *Geophys. J. Intl.*, *111*, 515-530.

Weller, M. B., & Lenardic, A. (2012, May). Hysteresis in mantle convection: plate tectonics systems. *Geophysical Research Letters*, *39*(10).

Xie, S., & Tackley, P. J. (2004). Evolution of U-Pb and Sm-Nd systems in numerical models of mantle convection and plate tectonics. *Journal of Geophysical Research*, *109*(B11), B11204.

Yamazaki, D., & Karato, S.-I. (2001). Some mineral physics constraints on the rheology and geothermal structure of earth's lower mantle. *American Mineralogist*, *86*(4), 385–391.

Zegers, T. E., & van Keken, P. E. (2001, December). Middle Archean continent formation by crustal delamination. *Geology*, *29*(12), 1083–1086.

Zerr, A., Diegeler, A., & Boehler, R. (1998, July). Solidus of Earth's Deep Mantle. *Science*, *281*(5374), 243–246.

References from Supporting Information

References

Bodinier, J. L., & Godard, M. (2003, Dec). Orogenic, Ophiolitic, and Abyssal Peridotites. *Treatise on Geochemistry*, *2*, 568. doi: 10.1016/B0-08-043751-6/02004

-1

Castro, A., & Gerya, T. (2008). Magmatic implications of mantle wedge plumes: Experimental study. *Lithos*, *103*(1), 138 - 148. Retrieved from `http://www.sciencedirect.com/science/article/pii/S0024493707002228` (Rocks Generated under Extreme Pressure and Temperature Conditions: Mechanisms, Concepts, Models) doi: https://doi.org/10.1016/j.lithos.2007.09.012

Cottaar, S., & Lekic, V. (2016, November). Morphology of seismically slow lower-mantle structures. *Geophysical Journal International*, *207*(2), 1122–1136.

Deschamps, F., Cobden, L., & Tackley, P. J. (2012). The primitive nature of large low shear-wave velocity provinces. *Earth and Planetary Science Letters*, *349*, 198–208.

Garnero, E., & McNamara, A. (2008). Structure and dynamics of earth's lower mantle. *Science*, *320*, 626–628.

Hernlund, J. W., & Houser, C. (2008). The statistical distribution of seismic velocities in Earth's deep mantle. *Earth and Planetary Science Letters*, *265*(3-4), 423–437.

Tackley, P. J. (2012, January). Dynamics and evolution of the deep mantle resulting from thermal, chemical, phase and melting effects. *Earth-Science Reviews*, *110*(1-4), 1–25.